Calhoun
Institutional Archive of the Naval Postgraduate School

Calhoun: The NPS Institutional Archive

DSpace Repository

Theses and Dissertations | 1. Thesis and Dissertation Collection, all items

1974

Measurements of early magnetic fields in laser produced plasmas.

Wegener, Bernd.

http://hdl.handle.net/10945/17121

Downloaded from NPS Archive: Calhoun

http://www.nps.edu/library

Calhoun is the Naval Postgraduate School's public access digital repository for research materials and institutional publications created by the NPS community. Calhoun is named for Professor of Mathematics Guy K. Calhoun, NPS's first appointed -- and published -- scholarly author.

Dudley Knox Library / Naval Postgraduate School
411 Dyer Road / 1 University Circle
Monterey, California USA 93943

MEASUREMENTS OF EARLY MAGNETIC FIELDS IN LASER PRODUCED PLASMAS

Bernd Wegener

DUDLEY KNOX LIBRARY
NAVAL POSTGRADUATE SCHOOL
MONTEREY, CALIFORNIA 93943

NAVAL POSTGRADUATE SCHOOL
Monterey, California

THESIS

MEASUREMENTS OF EARLY MAGNETIC FIELDS IN LASER PRODUCED PLASMAS

by

Bernd Wegener

June 1974

Thesis Advisor: A. W. Cooper

Approved for public release; distribution unlimited.

T 162 486

UNCLASSIFIED

SECURITY CLASSIFICATION OF THIS PAGE (When Data Entered)

REPORT DOCUMENTATION PAGE		READ INSTRUCTIONS BEFORE COMPLETING FORM
1. REPORT NUMBER	2. GOVT ACCESSION NO.	3. RECIPIENT'S CATALOG NUMBER
4. TITLE (and Subtitle) Measurements of Early Magnetic Fields in Laser Produced Plasmas		5. TYPE OF REPORT & PERIOD COVERED Master's Thesis June 1974 6. PERFORMING ORG. REPORT NUMBER
7. AUTHOR(s) Bernd Wegener		8. CONTRACT OR GRANT NUMBER(s)
9. PERFORMING ORGANIZATION NAME AND ADDRESS Naval Postgraduate School Monterey, California 93940		10. PROGRAM ELEMENT, PROJECT, TASK AREA & WORK UNIT NUMBERS
11. CONTROLLING OFFICE NAME AND ADDRESS Naval Postgraduate School Monterey, California 93940		12. REPORT DATE June 1974 13. NUMBER OF PAGES 83
14. MONITORING AGENCY NAME & ADDRESS (if different from Controlling Office) Naval Postgraduate School Monterey, California 93940		15. SECURITY CLASS. (of this report) UNCLASSIFIED 15a. DECLASSIFICATION/DOWNGRADING SCHEDULE

16. DISTRIBUTION STATEMENT (of this Report)

Approved for public release; distribution unlimited.

17. DISTRIBUTION STATEMENT (of the abstract entered in Block 20, if different from Report)

18. SUPPLEMENTARY NOTES

19. KEY WORDS (Continue on reverse side if necessary and identify by block number)

Laser Produced Plasmas
Self-Generated Magnetic Fields

20. ABSTRACT (Continue on reverse side if necessary and identify by block number)

A plasma was produced by irradiation of an aluminum target with a 280MW, 25 nsec pulse from a neodymium-doped glass laser. The resulting plasma expanded into an ambient background of 5×10^{-5} Torr to 1000 mTorr and was analyzed using floating double probes and magnetic probes. An early magnetic field was observed which arrived at the probe position before the main plasma.

DD FORM 1 JAN 73 1473 EDITION OF 1 NOV 65 IS OBSOLETE
S/N 0102-014-6601 | 1
(Page 1)

UNCLASSIFIED

SECURITY CLASSIFICATION OF THIS PAGE (When Data Entered)

Block #20 continued

The pressure dependence of the early magnetic signal was found to agree with the relationship $B_{\theta MAX} \propto \rho_0^{1/3}$. According to this dependence the early magnetic signal is thought to be due to the diffusion of the magnetic field generated during the early phase of illumination of the target by the laser.

The strong reversed field observed at the front of the laser plasma is attributed to the development of an axial electron temperature gradient due to snowplowing of the ambient plasma and to the larger radial density gradient.

Measurements of Early Magnetic Fields in Laser Produced Plasmas

by

Bernd Wegener
Lieutenant Commander, Federal German Navy

Submitted in partial fulfillment of the
requirements for the degree of

MASTER OF SCIENCE IN PHYSICS

from the

NAVAL POSTGRADUATE SCHOOL
June 1974

Thesis
W334
c.

DUDLEY KNOX LIBRARY

ABSTRACT

A plasma was produced by irradiation of an aluminum target with a 280MW, 25 nsec pulse from a neodymium-doped glass laser. The resulting plasma expanded into an ambient background of 5×10^{-5} Torr to 1000 mTorr and was analyzed using floating double probes and magnetic probes. An early magnetic field was observed which arrived at the probe position before the main plasma.

The pressure dependence of the early magnetic signal was found to agree with the relationship $B_{\theta MAX} \propto \rho_o^{1/3}$. According to this dependence the early magnetic signal is thought to be due to the diffusion of the magnetic field generated during the early phase of illumination of the target by the laser.

The strong reversed field observed at the front of the laser plasma is attributed to the development of an axial electron temperature gradient due to snowplowing of the ambient plasma and to the larger radial density gradient.

TABLE OF CONTENTS

I. INTRODUCTION..... 10

II. PREVIOUS EXPERIMENTAL WORK..... 12

A. SELF-GENERATED MAGNETIC FIELDS..... 12

B. EARLY TIME SIGNAL..... 14

III. THEORY..... 20

A. SELF-GENERATED MAGNETIC FIELDS..... 20

B. INTERACTION BETWEEN LASER PLASMA AND AMBIENT PLASMA..... 25

IV. EXPERIMENTAL ARRANGEMENT..... 29

A. LASER..... 29

B. LASER MONITORING TECHNIQUES..... 29

C. VACUUM CHAMBER..... 30

D. TEMPORAL REFERENCE FRAME..... 31

E. FLOATING DOUBLE PROBES..... 33

F. MAGNETIC PROBES..... 33

1. Probe Construction and Calibration..... 33

2. Probe Signal Integration..... 34

3. Probe Reliability..... 37

G. DATA COLLECTION ERROR ESTIMATES..... 38

1. Errors in Temporal Resolution..... 38

2. Errors in Probe Positioning..... 38

3. Probe Perturbations..... 38

V. INDIVIDUAL EXPERIMENTS AND THEIR RESULTS..... 40

VI. ANALYSIS OF EXPERIMENTAL RESULTS..... 48

VII. SUMMARY AND CONCLUSIONS..... 57

BIBLIOGRAPHY..... 80

INITIAL DISTRIBUTION LIST..... 83

LIST OF FIGURES

1. Block Diagram of Experimental Arrangement..... 59

2. Top View of Vacuum Chamber..... 60

3. Electric Double Probe Characteristic at the Peak of the Early Time Signal..... 61

4. Calibration Curve for the Magnetic Probe..... 62

5. Circuit Diagram for the Passive RC-Integrator..... 34

6. Removal of Electrostatic Pickup from Magnetic Probe Signal..... 63

7. Temporal Relationship Between Laser Pulse, Double Probe Signal and Magnetic Probe Signal (0.4,0,1.0)..... 64

8. Temporal Relationship Between Laser Pulse, Double Probe Signal and Integrated and Non-integrated Magnetic Probe Signal (0.4,0,1.0)..... 65

9. Early Time Signal from Double Probe in Different Nitrogen Background Pressures (0.4,0,1.0)..... 66

10. Magnetic Probe Signal in Different Nitrogen Background Pressures (0.4,0,1.0)..... 67

11. Pressure Dependence of Azimuthal Magnetic Field for Probe Positions (0.3,0,0.4) and (0.4,0,1.0)... 68

12. Temporal Relationship Between Laser Pulse, Electric Double Probe Signal and Magnetic Probe Signal in Vacuum for (0.6,0,2.5)..... 69

13. Electric Double Probe Signal for Different Background Pressures (0.6,0,2.5)..... 70

14. Magnetic Probe Signal for Different Background Pressures of Nitrogen (0.6,0,2.5)..... 71

15. Magnetic Field Strength as Function of Irradiance for Probe Position (0.6,0,2.5)..... 72

16. Maximum Early Magnetic Signal as Function of Nitrogen Background Pressure (0.6,0,2.5)..... 72

17. First Negative Magnetic Signal and Second Positive Magnetic Signal as Function of Nitrogen Background Pressure (0.6,0,2.5)..... 73

18. Negative Magnetic Signal Subtracted from Positive Magnetic Signal as Function of Nitrogen Background Pressure (0.6,0,2.5)..... 74

19. Early Magnetic Signal and Negative Magnetic Signal as Function of Background Pressure (0.6,0,2.5)..... 75

20. Negative Magnetic Signal Subtracted from Early Magnetic Signal as Function of Background Pressure (0.6,0,2.5)..... 76

21. Early Time Signal and Main Signal of Electric Double Probe as Function of Background Pressure (0.6,0,2.5)..... 77

22. Magnitude of Density Gradient in Radial and Axial Direction (0.4,0,1.0)..... 78

23. Magnitude of Density Gradient in Radial and Axial Direction (0.6,0,2.5)..... 78

24. Maximum Observed and Computed Values for B_{MAX} for the Early Magnetic Signal as Function of Background Pressure (0.6,0,2.5)..... 79

ACKNOWLEDGEMENT

I wish to thank Mr. Hal Herreman for his help and guidance and above all for the patience he has shown.

Special thanks to Professor Schwirzke who suggested this investigation and to Professor Cooper who took the time to help me in the interpretation of the results. This research was partially supported by the Office of Naval Research, project number 099-400; project order P04-0077.

I. INTRODUCTION

By focusing a giant-pulse laser onto a target a dense, energetic plasma can be produced by vaporization of some of the opaque target surface and subsequent absorption of laser light in this vaporized material.

Since the discovery of the Q-switch technique for lasers in 1962 and the subsequent development of high power lasers with nanosecond or picosecond pulse duration a considerable amount of research has been done on the subject of laser produced plasmas. A bibliographical review of the subject is given by DeMichelis [Ref. 1]. An introduction to the theoretical and experimental aspects of the subject is given by J. Ready [Ref. 2] and by P. Mulser, R. Sigel and S. Witkowski [Ref. 3].

Laser produced plasmas are of interest for a number of applications in physics and technology. It has been found that laser produced plasmas are an ideal spectroscopic light source, especially for the spectra of highly ionized gases. These plasmas also have found interest as electron and ion sources for particle accelerators. The initially high temperatures and densities of laser produced plasmas (called laser plasmas for short) make them of particular interest in the field of fusion research.

The discovery of self-generated magnetic fields in laser plasmas by Korobkin and Serov [Ref. 4] and by J. Stamper, K.

Papadopoulos, R. N. Sudan, S. O. Dean, E. A. McLean and J. Dawson [Ref. 5] led to more detailed investigations by McKee [Ref. 6] and Bird [Ref. 7]. The observed spontaneous magnetic fields are of the order of kilogauss which may have a considerable influence on laser plasmas in confinement experiments.

It was observed as early as 1963 that in front of the main body of the expanding plasma there is an early signal observed on particle detectors prior to the main signal [Ref. 8,9]. A detailed study of this early time signal was conducted by Brooks [Ref. 10]. Bird found during his experiments that there was an early magnetic signal too. Since his investigation did not include a study of this relatively weak magnetic signal this investigation has been conducted in an effort to ascertain that there is an early magnetic signal and to determine its relationship to the main magnetic signal and the early time signal as investigated by Brooks.

This thesis is divided into six more sections. Section II contains the previous experimental work concerning self-generated magnetic fields and work on the early time signal. Section III is a short presentation of the theory describing self-generated magnetic fields and a laser plasma interacting with an ambient plasma. Section IV contains the experimental arrangement. Section V presents the individual experiments and their results and Section VI is an analysis of the experimental results. Section VII gives a summary with conclusions.

II. PREVIOUS EXPERIMENTAL WORK

A. SELF-GENERATED MAGNETIC FIELDS

In 1971 the observation of spontaneously generated magnetic fields in laser plasmas was reported by J. A. Stamper, K. Papadopoulos, R. N. Sudan, S. O. Dean, E. A. McLean and J. Dawson [Ref. 5]. For most of their studies they used a Lucite fiber with 0.25 mm diameter as a target. The laser used was a neodmium-doped glass laser with an output of 60 joules in 30 nsec. A variety of magnetic probes were used to measure the spontaneous magnetic fields. The fields were measured in different background pressures of nitrogen and were found to be independent of the background pressure in the range from 50 to 200 mTorr. Fields of the order of kilogauss were observed.

The results of Stamper's experiment were taken by Chase, LeBlanc and Wilson [Ref. 11] to conduct an investigation to determine the effects of spontaneous magnetic fields on the evolution of laser produced deuterium plasma. This is of particular interest in the field of thermo nuclear fusion experiments. It was found that the spontaneous magnetic fields enhance the electron temperature and the production of neutrons. Computer simulation showed that in the presence of self-generated magnetic fields the maximum electron and ion temperatures are much higher and the region of high temperature is more concentrated than without fields.

Further research to determine the dependence of self-generated magnetic fields on position, time, incident laser power and ambient background pressure was undertaken by McKee [Ref. 5]. The target for these experiments was a 5 mil Mylar foil irradiated with a 300MW, 25 nsec laser pulse from a neodymium-doped glass laser. McKee reported that the strength of the magnetic field as well as its spatial and temporal dependences was found to be strongly dependent on the ambient background pressure. The following observations were made:

-- For a fixed position the maximum value of the magnetic field strength was increased by a factor of six when the nitrogen background pressure was increased from 1 mTorr to 200 mTorr.

-- The maximum field signals occurred earlier in time at a background pressure of 250 mTorr than at 0.1 mTorr.

-- The fields showed azimuthal symmetry around the target normal although the angle of incidence of the laser beam was 30°.

-- A small magnetic field in the opposite direction was found to occur after several hundred nanoseconds. For a background pressure of 250 mTorr the reversed field appeared sooner in time than for lower background pressure.

The pressure dependence of self-generated magnetic fields was further investigated by Bird [Ref. 7]. Bird irradiated a slab of aluminum with a 300MW, 22 nsec pulse from a neodymium-doped glass laser. In addition to magnetic probes,

electric double probes were used to study the spontaneous magnetic fields in a laser produced plasma expanding into backgrounds of different gases, in relationship to the plasma density profiles. The findings of this investigation were:

-- The shell model used by McKee to explain the pressure dependence of the self-generated magnetic fields does not agree with the results obtained by use of the electric double probe. No density shell was found in front of the Mylar laser plasma and also the reversed fields in front of an aluminum laser plasma expanding into a dense background could not be explained by this model.

-- A model which explains the results obtained in the investigation uses the interaction between photoionized background plasma and the laser plasma.

-- Reverse fields can be produced by causing the plasma front to decelerate rapidly. This can be done by placing a glass plate in the path of the expanding plasma.

B. EARLY TIME SIGNAL

To determine what causes the early signal preceding the main plasma body several hypotheses have been put forward. Among them are laser induced electron emission, fast plasma blowoff [Ref. 9] and ionization potential waves [Ref. 12]. At the Naval Postgraduate School, Monterey an investigation was undertaken by Brooks [Ref. 10] to determine the nature of the early disturbance. His research indicates that the

early signal is composed of electrons and ions. This result excludes the laser induced electron emission as source for the early disturbance. A review of the literature does reveal several reports to back up and explain his findings. Investigators using different target materials and laser power combinations have observed two ion current peaks when measuring the ion collector current signals for expanding plasmas [Ref. 13-16]. It was found that the fast ion peak contained high energy ions and that the slow peak contained ions of normal energy.

Bykovskii and others [Ref. 14] developed a mass-spectrometer for the investigation of ions formed by the interaction between laser radiation and matter. It was found that the energy distribution of ions depends on the size of their charge.

Further investigation by the same group [Ref. 15,16] led to the discovery of singly charged ions in the high energy region which consists mainly of highly charged ions. The presence of singly charged ions in the high energy region was attributed to recombination processes. A possible explanation for the dependence of the energy distribution on the ion charge was offered. It was assumed that this dependence was caused by acceleration of the ions in self-consistent electrostatic fields. These fields were thought to be created by electrons trying to leave the plasma due to their high thermal velocities. The ions moving in the resultant field are accelerated to velocities well in excess of their

thermal velocities. This acceleration is a function of the charge of the ions.

Similar research was conducted by Paton and Isenor [Ref. 7] who used a Ruby laser to irradiate gold, copper and aluminum targets with a pulse of about 25MW and 20 nsec duration. They found that if they assumed that the rapidly escaping electrons give up their energy by electrostatic interaction to the ions the resulting mean energy was of the form of $E_n = (n+1)kT$ where T is the initial plasma temperature and n is the charge multiplicity. They also found an increase in mean energy with the mass number of the target element.

Similar experiments executed by Demtroeder and Jantz [Ref. 18] using a Ruby Giant Pulse Laser with about 100MW peak power and 30 nsec halfwidth led to comparable results. They too used copper and aluminum targets. Using the same model in which the electrons leave the plasma and build up an electrostatic field the final kinetic energy of the ions with charge Ze could be equated to the initial thermal energy of the electrons and ions in the form of the following equation

$$E_{kin} = ZkT_e + kT_i. \qquad (1)$$

This equation predicts a temperature considerably above the observed values, which is due to the fact that the model leading to Equation (1) assumes that the laser energy has been transformed to thermal energy before the expansion of the plasma starts. Since heating and expansion take place

simultaneously the model gives temperatures which are too high. To explain the large difference between the large kinetic energy of the ions and their relatively low thermal energy it was assumed that the electrons can repeat the ion acceleration many times. From the observed final kinetic energies of the ions an average energy transfer rate from electrons to ions of about 25 x Z eV/nsec was deduced. The model proposed for that is that a fast electron leaving the plasma cloud returns because of the electrostatic attraction and transfers a fraction of its energy. The frequency at which this process has to be repeated leads to an oscillation frequency which was found to be lower than the plasma frequency at those plasma densities where heating and acceleration take place.

The fact that ions in a higher charge state escape earlier from the laser produced plasma than ions of lesser charge has been observed in several experiments. Allen [Ref. 19] used an electrostatic analyzer, Haught and Polk [Ref. 20] utilized a mass spectrometer and Irons, McWhirter and Peacock [Ref. 21] found the dependence of ion velocities on their charge by using spectroscopic measurements.

The model of electrostatic fields causing the separation of ions of different charge has been examined more closely by Mulser [Ref. 21]. His theoretical investigation set out to calculate the internal electric field and investigate its influence on ion separation. In the investigation recombination and charge exchange processes were neglected but the

friction between the ions of different charge was included. Mulser arrived at the result that the expansion velocities of differently charged ions are equal as soon as the friction is included. Therefore he concluded that ion separation by means of electrostatic fields contained in the interior of a laser plasma is not a correct model.

Allen [Ref. 23] drew the same conclusion from the investigation of a variety of experimental results but he proposed some alternative mechanisms which could account for the observed fact of ion separation.

Allen considered microscopic processes in the laser plasma which could account for the production of ions with high kinetic energies. He found that ion energies in the order of hundreds of eV to a few keV can be accounted for by collision processes between atomic sized particles. This means that kinetic energy and excitation energy are exchanged in collisions between unexcited ions and atoms and excited ions and atoms. Energy is also exchanged in collisions of excited ions with one another. The thermal energy of the electrons which extract the energy from the laser beam mainly by inverse bremsstrahlung is converted to excitation and ionization energy of the target atoms which then undergo the collisions as described above. But as Allen found one cannot account for the high ion kinetic energies by direct electron-ion collisions.

A more detailed study of the ionization processes has been completed by Stumpfel, Robitaille and Kunze [Ref. 24]. Their investigation based upon spectroscopic measurements

was conducted especially during the early phases of plasma production.

Consideration has to be given to an experiment conducted by Ehler and Linlor Ref. 25 . They used a 35MW ruby laser with a 20 nsec pulse width focused on a thick tungsten target in a vacuum chamber. Investigation of the fast and slow ion peak observed with an ion collector in different background pressures led to the conclusion that the fast ion peak consisted of ions of much lower mass than tungsten. It was also found that the fast ion originated from a large area on the target while the slow ions came from a small area at the focal center. The explanation offered by Ehler and Linlor was that the fast ion peak consisted of ions of impurities absorbed by the target surface. An attempt has not been made to explain all fast ion peaks which have been observed for a variety of targets by impurities but it is obvious that contamination of the target surface can lead to erroneous experimental results.

On the basis of Brooks' work the emphasis in this section has been on fast plasma blowoff as an explanation for the early time signal recorded with electric double probes. There are however other explanations like the ionization potential wave which describe a mechanism for the production of the early time signal.

III. THEORY

A. SELF-GENERATED MAGNETIC FIELDS

In 1966 Basov and others [Ref. 28] investigated the plasma produced by a giant laser pulse on a solid target. Parameters of this plasma, called a "flare" were obtained with the help of probes capable of determining the electron emission current and by high speed cameras. It was noted that the decaying flare emits electrons which create a current of the order of tens of amperes. It was deduced that these currents should be the source for magnetic fields in the laser produced plasma.

Stamper and others [Ref. 5] attributed the generation of the observed magnetic fields to thermoelectric currents. These currents were thought to be associated with a thermoelectric junction formed by the laser focus and the plasma.

The equation governing the development of spontaneous magnetic fields has been derived in some detail by Bird [Ref. 7] Stamper [Ref. 19] and Schwirzke [Ref. 30]. For completeness this basic equation is derived and the meaning of the different terms in pointed out.

Assuming a two-fluid model of electrons and ions of a collision dominated neutral plasma leads to the following linearized equations of motion:

$$n_e m_e \frac{\partial \vec{u}_e}{\partial t} = -n_e e(\vec{E}+\vec{u}_e x \vec{B}) - \nabla P_e + n_e m_e \nu_{ei}(\vec{u}_e - \vec{u}_i) \qquad (2)$$

$$n_i m_i \frac{\partial \vec{u}_i}{\partial t} = n_i e(\vec{E}+\vec{u}_i x\vec{B}) - \nabla P_i + n_e m_e \nu_{ei}(\vec{u}_e-\vec{u}_i) \qquad (2a)$$

$n_e m_e = \rho_e$ and $n_i m_i = \rho_i$ are the electron and ion mass density respectively, $\vec{u}_e$ and $\vec{u}_i$ are the fluid velocities of the electrons and ions, P_e and P_i are the pressures of the electrons and ions. The expression $n_e m_e \nu_{ei}(\vec{u}_e-\vec{u}_i)$ is a friction term due to the relative velocity between electrons and ions. Assuming single ionization only and also assuming quasi-neutrality $n_e = n_i = n$. Further considering that

$$\rho_e \nu_{ei}(\vec{u}_e-\vec{u}_i) = \frac{n_e m_e \nu_{ei}(\vec{u}_e-\vec{u}_i)e}{e}$$

$$= -\frac{m_e \nu_{ei} \vec{j}}{e} = \frac{n_e e \vec{j} \nu_{ei} m_e}{n_e e^2}$$

$$= -\frac{n_e e}{\sigma}\vec{j} .$$

Equations (2) and (2a) can be written as

$$\rho_e \frac{\partial \vec{u}_e}{\partial t} = -ne(\vec{E}+\vec{u}_e x\vec{B}) - \nabla P_e + \frac{en_e}{\sigma}\vec{j} \qquad (3)$$

$$\rho_i \frac{\partial \vec{u}_i}{\partial t} = ne(\vec{E}+\vec{u}_i x\vec{B}) - \nabla P_i \pm \frac{en_e}{\sigma}\vec{j} \qquad (3a)$$

where $\vec{j}$ is the current density and σ is electrical conductivity. After multiplying Equation (3) by m_i and Equation (3a) by m_e subtracting (3) from (3a) leads to

$$\vec{E}\left(\frac{1}{m_i}+\frac{1}{m_e}\right) + \frac{1}{m_i}(\vec{u}_i x\vec{B}) + \frac{1}{m_e}(\vec{u}_e x\vec{B}) - \frac{\nabla P_i}{nem_i} + \frac{\nabla P_e}{nem_e} - \frac{\vec{j}}{\sigma}\left(\frac{1}{m_i}+\frac{1}{m_e}\right)=0 \qquad (4)$$

Substituting m' for $1/m_i + 1/m_e$ and solving for E results in

$$\vec{E} = \frac{\vec{j}}{\sigma} - \frac{1}{m_i m'}(\vec{u}_i x \vec{B}) - \frac{1}{m_e m'}(\vec{u}_e x \vec{B}) - \frac{1}{n e m_e m'} \nabla P_e + \frac{1}{n e m_i m'} \nabla P_i . \quad (5)$$

Assuming $m_i >> m_e$, $1/m_i m'$ approaches zero and $1/m_e m'$ is approximately equal to one. Entering these approximations in Equation (5) leads to

$$\vec{E} = \frac{j}{\sigma} - (\vec{u}_e x \vec{B}) - \frac{1}{n_e e} \nabla P_e . \quad (6)$$

The same expression can be obtained assuming that during the heating phase of the plasma $T_e >> T_i$. This means that the ions are almost stationary during the initial phase and mainly the electrons react to the created solenoidal electric field. The scalar electron pressure is assumed since the velocity distribution within the volume of consideration is isotropic (i.e., electron-electron collision time is much less than the field production time). That means Equation (6) could be obtained using only the equation of motion for the electron fluid.

The equation describing the development of the magnetic field can be obtained by taking the curl of Equation (6) and combining the result with Maxwell's equations.

$$\frac{\partial \vec{B}}{\partial t} = - \nabla x \vec{E} \quad (7)$$

$$\frac{\partial \vec{B}}{\partial t} = \frac{1}{\sigma} \nabla x \vec{j} + \nabla x (\vec{u}_e x \vec{B}) + \nabla x \frac{1}{n_e e} \nabla P_e . \quad (8)$$

The term $- \frac{1}{\sigma} \nabla x \vec{j}$ can be rewritten by applying $\mu_0 \vec{j} = \nabla x \vec{B}$ and $\nabla \cdot B = 0$.

$$- \frac{1}{\sigma} \nabla x \vec{j} = \frac{1}{\mu_0 \sigma} \nabla^2 \vec{B}$$

which clearly constitutes a diffusion term. This means that the first two terms on the right hand side are the flow and diffusion terms and the third expression on the right hand side of Equation (8) is the term describing the generation of the magnetic field.

The flow term $\nabla x(\vec{u}_e x \vec{B})$ describes the convective transport of the magnetic field. When the magnetic Reynolds number is greater than 1 the flow term predominates over the diffusion term and the magnetic field lines move along with the velocity of the electron fluid, that is with the local plasma velocity.

The magnetic Reynolds number is defined as the ratio of the flow and diffusion terms and can be written as

$$R_m = \mu_0 \sigma L u$$

where L is an average length characteristic of the flow.

The diffusion term represents the conversion of field energy to internal energy through Joule heating. This mechanism is predominant for the case that the magnetic Reynolds number is much smaller than 1. That means B is not appreciably influenced by the plasma motion u. The diffusion time which is the decay time of the magnetic field due to ohmic losses is given by $\tau_m = \mu_0 \sigma L^2$.

The third term in Equation (8), representing sources for the generation of a magnetic field is of primary interest here and warrants closer examination. Assuming an equation of state for the plasma of the form $P_e = nkT_e$ the source term can be written according to Schwirzke [Ref. 30] as

$$\nabla x \frac{1}{n_e e} \nabla P_e = \nabla x \frac{1}{n_e e} \nabla (n_e k T_e) = \nabla x \left(\frac{k}{e} \nabla T_e + \frac{k T_e}{n_e e} \nabla n_e\right). \quad (9)$$

The temperature is a scalar and the density gradient is a vector which leads to a vector identity $\nabla x (a\vec{B}) = \nabla a \times \vec{B} + \nabla a \times \vec{B}$. Using this vector identity and the fact that the curl of a gradient is zero, Equation (9) can be simplified to

$$\vec{S} = \frac{k}{e} \nabla T_e \times \frac{1}{n_e} \nabla n_e \quad (10)$$

where $\vec{S}$ denotes the source term.

For an adiabatic expansion $T n_e^{1-\gamma} = \text{const.}$ the source term vanishes. Thus non-adiabatic conditions are required to generate spontaneous fields. The adiabatic condition implies that n and P are functions of T. Thus, the gradients are all in the same direction. For non-adiabatic conditions the temperature and density gradients are non-parallel.

Considering a planar target, density gradients can be found in both radial and normal directions. The same holds true for the temperature gradients. The largest temperature gradient can be found in the radial direction and the largest density gradient in the direction of the target normal. This combination of gradients generates a magnetic field in the azimuthal direction. Since the radial temperature gradient is due to the finite radial extent of the laser beam, the strongest temperature gradient can be expected near the edge of the focal spot. The expansion of the plasma away from the target is the cause of the density gradient. This indicates

that the largest density gradient can be expected in the front of the expanding plasma.

It must be pointed out that another source term for the magnetic field generation exists. Stamper and Tidman give a formal derivation of a source term due to radiation pressure [Ref. 31]. Radiation pressure is defined as the time average of the momemtum flow tensor for the electromagnetic field. Thus the pressure P can be broken up into $P = P_e + P_r$, where P_r is the radiation pressure. Radiation pressure produces a solenoidal electric field and must be included in Equation (8). That means that the radiation pressure P_r is added to P_e and also included in Equation (9) and therefore in the source term (Equation 10). Thus radiation pressure results in a non-thermal source which means that electromagnetic field energy can be converted directly to magnetic field energy. It has been found that radiation pressure sources are important at intensities above 10^{14} W/cm^2 for plasmas produced by a neodymium-doped glass laser.

B. INTERACTION BETWEEN LASER PLASMA AND AMBIENT PLASMA

During his investigation of self-generated magnetic fields associated with laser plasma McKee [Ref. 6] used a model developed by Dean, McLean, Stamper and Griem [Ref. 32] to explain the interaction between a laser plasma and an ambient background plasma. Dean found with the help of framing photographs an expanding luminous interaction front which had well-defined boundaries. The distance to which the front expanded

was found to be a function of the pressure of the ambient background gas. This dependence of the expansion velocity on the background pressure was taken to be an indication of interaction between the laser plasma and the ambient plasma. Shadowgraphy revealed a front thickness of 1-2 mm which is small compared to a binary-collision momentum mean free path. Since the dynamics of the laser plasma were found to be in agreement with a strong momentum-coupling model, a collisionless interaction model was proposed. One possible mechanism is the ion-ion two-stream instability in the presence of a magnetic field. The interaction front was thought of as a shell with increased density because the background ions are swept up by the luminous front and reach approximately the velocity of the front.

The model of collisionless interactions between inter-streaming ions was challenged by Wright [Ref. 33]. It was shown that the results of the experiments conducted by Dean, McLean, Stamper and Griem could be explained by collisional processes. Wright argued that for the region in which the measurements were taken, the plasma density is high enough to collisionally snowplow up the background plasma. However, the existence of the shell with enhanced density was not challenged.

Bird [Ref. 7] found no evidence for the density shell in his investigation. He found it difficult to explain the field reversal at the front of the plasma in terms of the density shell model. Bird used the explanation given by

Koopman [Ref. 34] to establish his model of interaction. An interaction front has been detected which decelerates with a dependence on background density. Deceleration was also dependent on time in a manner consistent with a momentum coupling between the laser plasma and the ambient background. It was concluded that the momentum transfer was caused by multi-Coulomb collisions between the two plasmas.

Thus, in this model, the ionized fraction of the background plasma was swept up by the leading edge of the expanding laser plasma. In that way the mass of the streaming plasma is increased and due to the law of conservation of momentum the expansion velocity will decrease. If a shell-like interaction region is assumed it not only contains the photoionization plasma mass swept up by the shell as it has expanded from the origin, but also a fraction of the laser plasma. The portion of the laser plasma is that part which has been decelerated by momentum transfer to the background plasma.

In this model it is assumed that a large part of the kinetic energy of the ambient plasma ions is converted to thermal energy. This occurs when the ambient plasma ions are captured within the interface region. The mechanism for the heating is ion viscous forces. Due to the deceleration or "pile-up" of the laser plasma behind the interface there will be strong viscous heating here too.

Since electron temperature and density gradients are of importance in the generation of spontaneous magnetic fields

the behavior of the electrons in this model has to be investigated too. Bird assumed that the ambient plasma electrons undergo compressional heating in the interface during the early stages of the expansion. The heating due to the "pile-up" which causes the production of the large axial ion temperature gradient is assumed to be transmitted to the electrons by electron-ion collisions.

This model now is good for the explanation of the observed field reversal at the front of the expanding laser plasma during later times. It also explains the dependence of the reversed field on the ambient pressure.

Since this model fits the observations made during this investigation it has been adopted to explain the interaction between laser plasma and ambient plasma.

IV. EXPERIMENTAL ARRANGEMENT

A. LASER

The laser used in this investigation was a Korad K-1500 Q-switched neodymium-doped glass laser system. The system consists of an oscillator laser (K-1) which generates the initial 25 nsec (full width at half power) pulse through Q-switching by a Pockels Cell. The output beam is then expanded by the expansion optics from the 0.5 inch diameter of the oscillator rod to the 0.75 inch diameter of the amplifier laser rod. The amplifier (K-2) amplifies the energy of the pulse. The arrangement of the laser system components is shown in Figure 1. The output of the laser system can be controlled by variation of the voltage applied to the flashlamps of the Nd oscillator and Nd amplifier laser. The range of obtainable energies is 3.5 to 12 Joules. The duration of the laser pulse is 25 nsec which gives a range of output powers from 150 to 450 MW. The laser focal spot size is approximately 1.5 mm. This gives a power density of 3.9×10^9 watts/cm^2 for the energy of 7 Joules.

A more detailed description of the laser system is given in the MS Thesis of Davis [Ref. 26].

B. LASER MONITORING TECHNIQUES

In order to diagnose the laser beam a Korad K-D1 photodiode was used. Approximately 1% of the beam was reflected by a glass slide used as beam splitter to a MgO diffusor

block. The output is monitored from this block by the K-D1 photodiode after passing through a 0.1 percent density filter. The photodiode provides two signals, one proportional to the pulse power, the other proportional to the laser pulse energy. The photodiode energy signal was calibrated using a Korad K-J3 Laser Calorimeter. The calorimeter was used to provide an absolute measure of the incident laser pulse energy against which the voltage reading on the Tektronix 564B storage oscilloscope, which was used to display the energy signal, could be calibrated.

The power output signal was used to trigger a Tektronix 7904 oscilloscope and could also be displayed on that oscilloscope using the negative input in a differential amplifier. The energy output was monitored on every shot. The pulse width which was more reliable was checked before and after each series of measurements.

C. VACUUM CHAMBER

The target used was a disk of one-half inch 6061 aluminum alloy plate. The target diameter was two inches and the target could be rotated after 20 to 30 shots to avoid excessive cratering. However as has been shown by K. M. Brooks [Ref. 10] the cratering does not influence the expansion dynamics of the plasma.

The target was located in a vacuum chamber as shown by Figure 2. The chamber allows diagnosis of the laser produced plasma by optical means or with probes. The laser beam

entered the chamber after passing through a 28 cm focal length lens. Angle of incidence on the target was 30°, which allowed a probe to be positioned along the z-axis at radial distances from 4mm upward without having the laser beam strike and thereby damage the probe. Bringing the laser beam in at this angle results in expansion of the early plasma in the direction of the reflected laser beam [Ref. 10]. The main plasma however expands in the direction of the target normal.

The chamber could be pumped to a vacuum of 5×10^{-5} Torr (air) by an oil diffusion pump. The vacuum reached by Brooks (2.5×10^{-5} Torr) could not be achieved, since two probe holders instead of one were used. This increased the number of possible leaks.

For experiments requiring an ambient background for the laser produced plasma nitrogen gas could be admitted to the chamber. The ambient pressures of nitrogen gas used were 0.1 to 1000 mTorr.

Vacuum pressures lower than 10 mTorr were measured with an ionization gauge; higher pressures had to be measured by means of a thermocouple gauge, which was calibrated to the ionization gauge when the transition from one to the other had to be made.

D. TEMPORAL REFERENCE FRAME

Since two probes were used and the probe responses displayed on two separate oscilloscopes (Tektronix 7704 and

Tektronix 7904) both signals had to be calibrated to a common time frame. This was complicated by the fact that the two oscilloscopes have different response times. A common trigger source for both oscilloscopes could not be used, since the oscilloscope displaying the double probe signal and its trigger source had to be isolated from ground so that the probe was floating with the plasma potential. That was not the case for the magnetic probe. To achieve this, the trigger source for the Tektronix 7704 oscilloscope displaying the double probe response was a PIN diode with no ground connection. As trigger source for the Tektronix 7904 displaying the magnetic probe response the Korad K-D1 photodiode was used. Measurements showed the rise times of both photodiodes to be the same.

The power signal from the K-D1 detector was displayed simultaneously on both oscilloscopes and the leading edge of the pulse was taken as zero reference. Since the length of the coaxial cable from the K-D1 detector to the oscilloscope and the length of the coaxial cables from the magnetic probe and from the double probe to the oscilloscope were the same, no cable-induced delay existed between the signals. Considering that the optical path lengths between the beam splitter and the photodiode and between beam splitter and target are the same, zero time is established as that time at which the leading edge of the laser pulse strikes the target.

Exchanging the trigger sources for the oscilloscopes did not alter the established zero time line neither did an exchange of the input.

To make sure that no horizontal drift had occurred the timing was checked after every twenty to thirty shots. It was found that it stayed stable.

E. FLOATING DOUBLE PROBES

Probe construction and calibration is covered by Brooks [Ref. 10]. The primary use of the floating double probe was to determine the time at which the early time signal arrived at the magnetic probe and the duration of the early disturbances.

The characteristic of the probe was determined for the peak density of the early time signal and is reproduced in Figure 3. The characteristic was measured in a background of 5.0×10^{-5} Torr with a laser energy of 7 ± 0.7 joules. The probe was biased at -20 volts to collect a saturated ion current.

A more detailed description of probe theory and probe construction is given by Brooks [Ref. 10].

F. MAGNETIC PROBE

1. Probe Construction and Calibration

To diagnose the self-generated magnetic fields a small glass-enclosed inductive magnetic probe was used. Following the procedures outlined by McLaughlin [Ref. 27] the probe was calibrated by inserting it into carefully wound

Helmholtz coils. The effective area of the inductive loop nA was determined as $5.1 \times 10^{-6} m^2$.

For meaningful measurements of the self-generated magnetic fields the probe response has to be linear in the frequency range of interest. The magnetic probe used was found to have a linear response for frequencies up to 25 MHz and to have resonant frequencies of about 45 MHz. (See Figure 4.)

2. Probe Signal Integration

The response of the magnetic probe is an induced voltage V_p which is given by

$$V_p = nA\frac{dB_\perp}{dt} \tag{11}$$

where nA is the effective area of the probe coil and $dB_\perp/dt$ is the time rate of change of the component of the magnetic field normal to the plane of the coil. For equation (11) to be valid it has been assumed that the magnetic induction over the coil area is constant.

As shown by Equation (11) the probe response is proportional to dB/dt. In order to get signals proportional to the magnetic field itself the output of the probe has to be integrated over the time. This was done with a passive RC integrator shown in Figure 5.

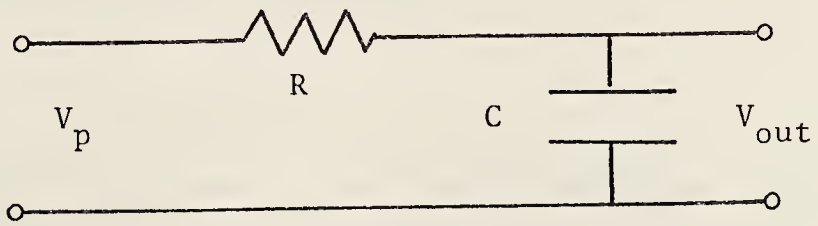

Figure 5.

V_p represents the output voltage of the inductive magnetic probe and V_{out} represents the voltage signal of the integrated output from the RC integrator. V_{out} is given by

$$V_{out} = \frac{1}{C} \int_0^t i(t')dt' \tag{12}$$

where i is the current in the circuit passing through R and is given by $(V_p - V_{out})/R$.

The output voltage of the magnetic probe which is the input voltage signal to the RC integrator is of the form $V_p = V_{po}e^{-i2\pi ft}$. V_{out} will be much smaller than V_p if RC is large compared to the integration time which simplifies Equation (12) since $(V_p - V_{out})/R$ goes to V_p/R.

$$V_{out} = \frac{1}{RC} \int_0^t V_p \, dt. \tag{13}$$

In order for that to be exact, i.e., the error introduced to be smaller than 5%, t/RC has to be smaller than 0.1 or in other words the time constant has to be more than 10 times the observation time t.

The input signal is from a magnetic probe so that

$$\int_0^t V_p dt = nAB. \tag{14}$$

That leads to the relationship

$$V_{out} = \frac{nA}{RC} B. \tag{15}$$

The lowest frequency f_o for which the above equation is considered valid is $2\pi f_o RC \geqq 10$. If this requirement is satisfied

Equation (15) can be applied to any signal which has a fundamental frequency not lower than f_o.

Since the frequencies for the magnetic field during the time of the early time signal were not known several dB/dt signals were integrated by graphical means and it was found that the lowest frequency was between 10 and 12 MHz. In this frequency range the response of the inductive magnetic probe was linear with an effective area of $5.1 \times 10^{-6} m^2$. Since the duration of the early time signal did not exceed 100 nsec lower frequencies than 10 MHz were not expected. The rise time for the magnetic probe can be determined by evaluating the probe response. The probe response was linear up to 25 MHz. Since the probe input was a sine wave $\tau/4$ has been chosen to represent the rise time. This results in a rise time of 10 nsec which is shorter than all rise times encountered in this investigation.

To get an acceptable signal size an integrator time constant of $RC = 2 \times 10^{-7}$ sec was used. Then $2\pi f_o RC = 12.6$ and the time constant was acceptable. The conversion factor between the magnetic field and the output of the RC integrator becomes than

$$B = 0.39\ V$$

where B is in Gauss and V is in millivolts.

For the probe position (0.6,0,2.5) the lowest frequency observed was 5 MHz. Therefore an integrator with a time constant of $RC = 4 \times 10^{-7}$ sec was used which led to a conversion factor $B = 0.78\ V$ where B is in Gauss and V is in millivolt.

3. Probe Reliability

To insure a meaningful magnetic signal several steps were taken. The target in the vacuum chamber was removed and the laser beam was allowed to pass through the chamber with the probes placed at the same coordinates for which measurements would be taken. It was found that no electrostatic noise pickup was recorded. Then the target was replaced and a probe signal recorded, after which the probe coil was turned 180° and the signal was compared with the previous signal to find out if it reversed polarity. It was found that a change in polarity occurred but that part of the signal was electrostatic in origin. To eliminate this electrostatic signal (which was not noise since it was reproduced with every shot) the following method was used.

After recording a signal the probe coil was turned 180° and a second signal was taken at the same probe position with the same pulse energy. Then the second signal was subtracted graphically from the first signal. If the magnetic signal is called m and the electrostatic signal is e then the first signal is e+m and the second is e-m which gives after (e+m)-(e-m) = 2m a magnetic signal twice as large as the recorded signal but without the electrostatic signal. (Figure 6.) Further, the signals obtained with the passive RC integrator were compared with those obtained by direct graphical integration of the dB/dt signal. It was found that the signals were comparable.

G. DATA COLLECTION ERROR ESTIMATES

1. Errors in Temporal Resolution

The time resolution in these experiments can be considered good. At a background density of 5×10^{-5} Torr the expansion velocity of the plasma is almost constant. Temporal measurements and comparisons are made with a horizontal scale of 20 nsec for the magnetic probe signals which allows interpretation of results to within 1 to 2 nsec. The floating double probe measurements are made with a horizontal scale of 50 nsec per division which allows an interpretation of the measurements within 5 nsec. That means an error for the time of duration of the early time signal of only 5%.

2. Errors in Probe Positioning

Since all measurements were made at two probe positions and the probes were not moved between measurements no errors could be introduced. The magnetic probe was introduced through the top of the vacuum chamber and its position could be determined with the help of a millimeter grid attached to the top of the chamber. This was accurate within 0.5 mm. Deviation in the magnetic signal could be introduced when the probe coil was rotated since it was found that the probe was not completely symmetric.

3. Probe Perturbation

Due to the external probe diameter of four millimeter for the magnetic probe the probe is the cause of some disturbance in the plasma which can lead to measurable

deviations from the correct results. The weak negative magnetic fields observed at the beginning of the magnetic probe signal (Figure 10) can be attributed to probe perturbations. The relative values obtained with the magnetic probe however should not be influenced by probe perturbations.

V. INDIVIDUAL EXPERIMENTS AND THEIR RESULTS

The first set of measurements was made in an effort to determine if the early magnetic probe signal found by Bird [Ref. 7] was a signal due to a magnetic field connected with the early time signal or if it was caused by electrostatic pickup.

For this purpose it was necessary to record both the magnetic probe signal and the floating double probe signal at the same position for the same laser pulse.

The position had to be chosen in such a way that the early time signal from the electric double probe was clearly discernible from the main plasma signal. This was found to be the case for a position 1 cm away from the target in the direction of the target normal.

The magnetic probe was inserted through the port on top of the vacuum chamber and positioned in such a way that the probe coils were normal with respect to the azimuthal magnetic field lines. The electric double probe was inserted through port 6 of the vacuum chamber (see Figure 2). This probe was located at the same radial distance as the magnetic probe but about 2 mm further in the z-direction. The construction of the probe holder allowed only a limited number of positions at which both probes could be located. For this reason a radial distance of 4 mm had to be chosen which does not give the maximum magnetic signal at this position ($z = 10mm$, $r = 4mm$, $\theta = 0°$).

To determine if there is a shielding effect on the double probe due to the magnetic probe in front of it, several shots were recorded with the magnetic probe removed and compared with double probe signals with the probe in place. It was found there is no difference in the onset and duration of the double probe signal. There was a difference in the region of ±5% in the magnitude of the early time signal. This difference however could also have been induced by differences in the laser pulse.

Since no information was available on the expected frequency range of the early magnetic signal the first measurements taken were $\partial B/\partial t$ - signals. A typical trace and its temporal relationship to the laser pulse and the double probe signal is shown in Figure 7.

In order to distinguish the magnetic signal from the electrostatic pickup the probe coils were turned 180°. To eliminate the electrostatic pickup the second magnetic signal was subtracted graphically from the first one which resulted in a trace as in Figure 7(d). A graphical integration of this signal showed that frequencies lower than 10 MHz could not be expected during the time period of interest. That led to the construction of a passive RC-integrator with a time constant of 2×10^{-7} sec. A comparison between the B-signals obtained by the graphical method from the $\partial B/\partial t$ signal and that obtained by the passive integrator showed complete agreement. A typical B-signal and its temporal

relationship to the laser pulse and the double probe signal is shown in Figure 8.

It must be noted that the same procedure as described for the $\partial B/\partial t$ signal has been used to eliminate electrostatic pickup. All measurements were taken at least three times and the results averaged to remove the influence of noise.

As can be seen from Figure 8 there is no clearly separated magnetic field connected with the electrical early time signal. The peak which occurs at 110 nsec is the magnetic signal from the main plasma. There is however a small hump on the magnetic signal trace at about 80 nsec which occurred with all measurements taken and could be interpreted as the peak of the magnetic signal from the early disturbance.

The small negative signal at the beginning also occurred in all measurements. It does not disappear nor change its general shape when several measurements are averaged and can therefore not be explained as noise. A possible explanation is offered by probe perturbations. At this time only one magnetic probe was in working condition since a second probe under construction could not be finished due to cessation of glass blower services. Several vacuum leaks appeared in the probe and the successive steps taken to stop these leaks enlarged the external diameter of the probe from two to four millimeters. A probe with this relatively large external diameter constitutes an obstacle to the plasma flow. The investigation by Bird led to the discovery that negative magnetic fields occur when a plasma encounters an obstacle.

Therefore this would offer a possible explanation for the occurrence of the weak negative B-signal.

The next set of experiments was intended to determine the influence of different background pressures on the form and size of the double probe signal and the magnetic signal. The gas used to increase the background pressure was nitrogen as used by McKee and Bird and the pressure was increased from 5×10^{-5} Torr to 1 Torr in steps of the same size as used by these investigators.

The development of the shape of the electric early time signal is shown in Figure 9 and that of the magnetic signal is shown in Figure 10. The measurements shown in these figures were taken at 0.5 mTorr, 50 mTorr and 500 mTorr nitrogen background pressure. It should be noted that the hump which could be the early magnetic signal does not disappear but becomes more pronounced with rising background pressure. The weak negative signal at the beginning of the trace disappears between 0.5 and 1 mTorr of background pressure. The onset of the positive B-signal which occurred in vacuum at 55 nsec occurs at 10 nsec for pressures of 1 mTorr and higher. Brooks [Ref. 9] found from time of flight measurements that the flow speed of the Early Disturbance is 1.1×10^{8} cm/sec. Since the distance between focal spot and probe in this experiment is 1.16 cm the arrival of the early plasma signal at the electric double probe after 10 nsec does agree with the speed determined by Brooks. It also agrees with the earlier arrival of the magnetic signal at

higher pressures. It shows that the magnetic field strength during the early time becomes strong enough to neutralize the weak magnetic signal found for expansion of the laser plasma into vacuum.

Plotting the magnitude of the main magnetic signal against background pressure yields a dependence similar to that found by McKee and Bird. For comparison the pressure dependance obtained by McKee for position (0.4,0,0.4) and the pressure dependence found during this investigation for position (0.4,0,1.0) are shown in Figure 11.

However, all further investigation at this position does not lead to conclusive results regarding the early magnetic signal. Obviously the magnetic signal from the main plasma and the magnetic signal from the early disturbance interact with each other. Therefore it is necessary to choose a position where the early disturbance is completely separated from the main plasma.

Such a position was found at z = 25mm, with a radial distance of 6mm and $\theta = 0°$. Since the observed frequency range of the magnetic signal was found to have 5 MHz as its lowest frequency a new passive integrator was chosen with a time constant of 4×10^{-7} sec. A typical magnetic signal and its relationship to the electric double probe signal and laser pulse is shown in Figure 12.

It is not obvious from the temporal relationship shown in Figure 12 that the early magnetic signal is connected with the early signal from the electric double probe. A better conclusion can be drawn from Figures 13 and 14 which show

the development of the magnetic signal and the double probe signal in different background pressures of nitrogen.

The onset of the first positive signal from the double probe occurs at 20 nsec. Assuming a speed of 1.1×10^8 cm/sec for the first early signal it should arrive at 21 nsec at the probe position. Therefore the first positive double probe signal can be identified as the early time signal. Defining the first positive signal from the magnetic probe as the early magnetic signal the dependence of this signal on incident laser power and background pressure is investigated.

Figure 15 shows the dependence on the incident laser power and Figure 16 the dependence on background pressure. It is obvious that the pressure dependence of the early magnetic signal is different from the relationship found previously for the main signal.

However, the influence of the negative magnetic signal following the early magnetic signal has to be considered. Assuming that a negative signal eliminates or weakens a positive signal which would have been in its place the relationship between both has to be investigated. In Figure 17 the maximum positive magnetic signal and the maximum negative signal which follows the early magnetic signal are plotted against different background pressures. Combining both signals in such a manner that the negative signal is subtracted from the positive signal results in a curve which is shown in Figure 18. This pressure dependence is almost

identical to that found for position (0.4,0,1) which is shown in Figure 11. The same operation performed for the Early Magnetic Signal and the negative signal whose relationship is shown in Figure 19 gives the result shown in Figure 20.

The peaks of the early magnetic signal and the negative magnetic signal are separated in time by about 175 nsec. Figure 14 shows that this separation in time stays constant up to 50 mTorr of nitrogen background pressure. Beyond this pressure the separation in time between the peaks becomes larger. The peak of the early magnetic signal appears to arrive at the probe position about 250 nsec after the leading edge of the laser pulse hits the target. This time of arrival does not seem to be influenced by the nitrogen background pressure. The peak of the negative magnetic signal however, which for vacuum arrives at about 400 nsec at the probe position arrives 200 nsec later for 250 mTorr background pressure.

Considering Figure 19 it appears as if there is no negative field in pressure range from about 2.5 to 40 mTorr. A possible explanation would be that for background pressures from about 0.1 to 50mTorr the negative magnetic signal does not become much stronger and that the early magnetic signal and the following positive magnetic signal both interact in such a way with the negative signal that it seems to disappear between 2.5 and 40 mTorr. Closer examination of Figure 14 however shows that there still could be a negative magnetic field which only is masked by the preceeding and

following positive fields. For higher background pressures the influence of the early magnetic field is obviously superseded by the influence of the second positive field. It does not appear as if the negative magnetic field only exists over a small range of pressure, however there is a pressure range where the influence of the preceeding and following fields dominates.

VI. ANALYSIS OF EXPERIMENTAL RESULTS

For the probe position (0.6,0,2.5) generation of a strong reversed magnetic field occurs as shown by Figure 12. The source term arrived at in section III (Equation (10)) does not account for the existing temperature gradients in the z-direction and the density gradients in the radial direction. It has been assumed that these gradients are small compared with the density gradient in the z-direction and the temperature gradient in the radial direction and could be ignored. The source term can be rewritten in scalar form if one takes all gradients into account.

$$S = \left[\frac{k}{e}\frac{\partial T_e}{\partial r} \quad \frac{1}{n_e}\frac{\partial n_e}{\partial z} \right] - \left[\frac{k}{e}\frac{\partial T_e}{\partial z} \quad \frac{1}{n_e}\frac{\partial n_e}{\partial r} \right]. \qquad (16)$$

Thus for a reversed magnetic field to occur the second term in Equation (16) has to be bigger than the first one. That means that the cross product responsible for the generation of reversed magnetic fields is

$$\frac{\nabla_z kT_e}{e} \times \frac{\nabla_r n_e}{n_e} .$$

Using the interaction model described by Bird in his investigation, field reversal can be explained in the presence of a sufficiently strong background plasma. In this case there occurs viscous heating in the interaction region which results in large axial temperature gradients in the ion fluid which

will be transmitted to the electrons via collisions. The field reversal observed in Figure 12 starts about 180 nsec after cessation of the laser pulse. Since the large radial temperature gradient is driven by laser radiation it can be expected that this gradient decays due to electronic heat conduction after cessation of the laser pulse. To determine the relative magnitude of the radial and axial density gradients as a function of time an examination of the density contours drawn by Brooks was conducted. The result for the probe position (0.6,0,2.5) is shown in Figure 23. Surprisingly the radial density gradient is the dominant one for this position. That leads to the conclusion that the second term on the right hand side of Equation (16) is larger than the first term, i.e., the source term is dominated by the cross product responsible for the generation of reversed magnetic fields.

However Figure 12 represents a probe signal in vacuum and therefore it is not obvious that the axial temperature gradient is larger than the radial temperature gradient even if the latter has decayed due to heat conduction. Closer examination of Figure 12 (double probe signal) reveals however that the main plasma does not expand into vacuum but into the tail of the early time signal. If this tail contains ions slowed down to a speed even slightly smaller than that of the main plasma the interaction with these particles should result in a noticeable increase of the axial temperature gradient.

It has to be noted that the relative magnitudes of axial and radial temperature gradients in Figure 23 are only valid for the expansion into vacuum. No density contours for different background pressures are available. It also has to be considered that the laser energy used in Brook's investigation was 5 Joules compared with 7 Joules for this investigation. It is assumed however that the relative magnitude of the gradients does not change considerably so that the source term causing the generation of negative fields is the dominant one.

This explanation also agrees with the results obtained for the position (0.4,0,1.0) which are shown in Figures 8 and 10. The only reversed magnetic field here is recorded in Figure 8(d) and 10(a) and could be explained by probe perturbation. For this position the axial density gradient is larger than the radial density gradient and also during the first 80 nsec of the magnetic signal the laser beam is still on. This means that the radial temperature gradient is the larger one which then results in the generation of positive magnetic fields. For rising background pressure it can be observed that the hump on the magnetic signal which occurs between 60 and 80 nsec gets more pronounced. Figure 10(b) shows clearly that due to the rising background pressure the axial temperature gradient is rising, which causes the second term on the right hand side of Equation (16) to grow. Since the laser beam has not ceased to irradiate the target the axial temperature gradient does not outgrow the radial

temperature gradient but weakens its contribution to the positive field generation.

The positive magnetic signal following the negative one in Figure 12 is caused by the source terms which are not influenced by the interaction region and therefore are not dominated by the axial temperature gradient.

Figure 23 also reveals that the radial density gradient is smaller for later times than the axial density gradient which can only lead to the conclusion that for this time period the source term for the positive magnetic fields in the stronger one.

The early magnetic signal preceeding the negative signal in Figure 12 can also be explained by the model used in this investigation. Assuming the early time signal recorded with the electric double probe to consist of fast blow off material, i.e., fast ions and electrons, most of their energy would be kinetic energy and not thermal energy. This leads to the conclusion that the particles between the fast plasma and the following main plasma have less kinetic energy but higher thermal energy. The observations made by Brooks lead to a further assumption. Brooks found in his investigation that the early time signal does not expand in the direction of the target normal but in the direction the incident laser beam would be reflected. It is therefore safe to assume that the fast blow off material moves in a more or less directed stream and does not expand spherically. Assuming an ambient plasma of uniform temperature results in

an axial temperature gradient which is growing from the onset of the early disturbance until it reaches the interaction region of the main plasma. If the early disturbance is generated during the time the laser is still irradiating the target, as is obvious from Figure 7, and the early magnetic field is generated by the same density and temperature gradients responsible for the positive magnetic field, then the relationship $B_{\theta MAX} \propto \rho_0^{1/3}$ as found by Bird should be valid.

Figure 24 shows a comparison between the computed and the observed values. Obviously there is a good agreement between computed and observed values up to 2.5-5 mTorr. For pressures larger than 5 mTorr the observed values are very much smaller than the computed values. An explanation is given by the influence of the following negative magnetic field which will weaken the positive early magnetic signal.

An attempt was made to determine the influence of the positive and negative magnetic fields on each other. Figure 18 which gives the difference between the second positive magnetic signal and the negative magnetic signal shows a good agreement with the curves for pressure dependence found by previous investigators [Ref. 6,7]. Similar subtraction of the early magnetic signal and the negative signal resulted in Figure 20. All that can be deduced from Figure 20 is that assuming the same pressure dependence as shown in Figure 11 a strong influence of the negative field occurs at about 10 mTorr background pressure.

The relationship between positive and negative fields found by this method is far from accurate, since no allowance has been made for the temporal relationship of positive and negative signal. Even if no conclusive results can be obtained from Figures 18 and 20, they show however that there is a relationship between the positive and the negative fields which must be taken into account.

The good agreement of the computed curve with the observed values in Figure 24 leads to some conclusions about the nature of the early magnetic field. The relationship observed by Bird that $B_{\theta MAX} = \rho_0^{1/3}$ is only expected to be valid during laser illumination of the target. There are two possible explanations for this phenomenon. The first is that the fields created during the time of illumination of the target by the laser are frozen into the plasma expanding during this early phase. For this to happen, the plasma with the magnetic field frozen into it has to move faster than the main body of the plasma, as can be clearly seen from Figures 12 and 14. The early magnetic signal arrives at the position (0.6,0,2.5) earlier than the main plasma. That could mean that the early magnetic signal is connected with the early signal observed on the floating double probe. On the other hand if the early magnetic signal were frozen into the fast plasma blow off it would indicate that the convective flow term in Equation (8) is the dominant term and that the diffusion term is negligible. This calls however for high temperatures of the plasma which

does not apply for the fast plasma blow off. As stated before, most of the energy in the fast early disturbance is thought to be kinetic energy and not thermal energy. Considering these points it does not seem possible that the early magnetic signal is a field frozen into the fast plasma blow off.

The second explanation considers the possibility of diffusion. McKee found that the plasma temperature during the absorption of the laser radiation reaches about 100 eV. This was the maximum temperature reached and it occurred a few nanoseconds after the arrival of the maximum laser energy at the target. However, during the initial phase of the absorption of the incident laser radiation the plasma temperature will be much less than the estimated 100 eV. This indicates that the spontaneous magnetic fields created early in the absorption pahse are strongly influenced by the diffusion term $\mu_0 \sigma \nabla^2 B$ on the right hand side of Equation (8). This diffusion term cannot be neglected when the temperature T_e is low since σ is a function of T_e. It means that the magnetic field generated during the early absorption phase will rapidly diffuse from the production region into the ambient background.

The generation of these fields during the early phase of laser illumination is covered by the source term

$$S = \frac{k}{e} \nabla_r T_e \times \frac{1}{n_e} \nabla_z n_e .$$

Assuming that the term $\frac{1}{n_e} \nabla_z n_e$ can be approximated by $\bar{V}_{LP}^{-1}$ where V_{LP} is the average expansion velocity of the laser plasma during the time the laser illuminates the target, the source term can thus be rewritten as

$$B_{\theta MAX} \propto \frac{\nabla_r k T_e}{e V_{LP}} . \qquad (17)$$

Observations made by Dean and others [Ref. 32] show that the expansion velocity of the plasma during laser illumination is dependent on the ambient pressure. The relationship found is $\bar{V}_{LP} \propto \rho_0^{-1/3}$. Thus from Equation (17) the dependence $B_{\theta MAX} \propto \rho_0^{1/3}$ can be predicted.

Dean suggested that the dynamics for the expansion of the laser plasma during the time of laser illumination follows that of a radiation driven detonation wave and for later times that of a blast wave model.

The dependence of the expansion velocity on the ambient pressure is in agreement with this model. If this model is accepted there should be a primary expansion of the laser plasma during the early phase of the laser illumination in the direction of the incident laser pulse. This has not been observed. It has to be considered however that the time during which a laser supported detonation wave could exist is relatively short since cutoff of the laser radiation occurs shortly after the leading edge of the laser pulse hits the target.

Thus the region for the generation of early magnetic fields is not expected to expand very far so that the source for the fields which then diffuse can be considered almost as a point source. That would account for the occurrence of early magnetic fields in a direction other than that of the incident laser beam.

This explanation agrees with observations made by Bird that the magnetic signals arrive at the probe position before the main plasma. Bird did not specify a preferred direction for this occurrence. It also explains why there is no peak in the early magnetic signal corresponding to the density peak of the fast plasma blow off. It does not completely rule out the possibility that there may exist temperature and density gradients throughout the fast plasma blow off and the following tail, but it is assumed that the fields generated by these gradients are weak compared with the diffused fields.

VII. SUMMARY AND CONCLUSIONS

The experiments conducted in this investigation and their results show that there exists an early magnetic field, as observed by other investigators. This early magnetic field is thought to be due to the diffusion of the magnetic field generated during the early phase of illumination of the target by the laser. No evidence has been found that the fast plasma blow off contains density and temperature gradients strong enough to generate measurable spontaneous magnetic fields. The possibility that the early magnetic field is a field due to diffusion of the magnetic field contained in the main plasma after cessation of the laser pulse has been ruled out since that would not lead to the excellent agreement between computed and observed data as shown in Figure 24. It has also been ruled out because the field generated in the front section of the expanding plasma is a strong negative field and the early magnetic signal is positive.

The negative field observed is attributed to the interaction of the expanding main plasma with the tail of the fast plasma blow off. This tail is though of as ions slowed down from the fast blow off and ions produced by the interaction of the fast plasma blow off and the ambient background. The interaction of the main plasma with this tail leads to a large increase of the axial temperature gradient whereas the

radial temperature gradient becomes smaller after cessation of the laser pulse. Together with the increase of the radial density gradient over the axial density gradient this leads to the dominance of the source term for a reversed magnetic field.

All results of this investigation support the interaction model described by Bird. As far as the conclusions about the origin of the early magnetic signal are concerned more could be said if the plasma temperature T_e could be mapped the way Brooks mapped the density contours of the expanding plasma. Such contour maps would reveal to what extent temperature and density gradients exist in the fast plasma blow off. It would also allow a good estimate about the importance of the diffusion term.

A complete mapping of the early magnetic signal would reveal if there is any preferred direction for which the diffusion takes place. Expecially the development of the early magnetic signal shortly after the leading edge of the laser pulse hits the target could lead to conclusions about the validity of the model used in this investigation.

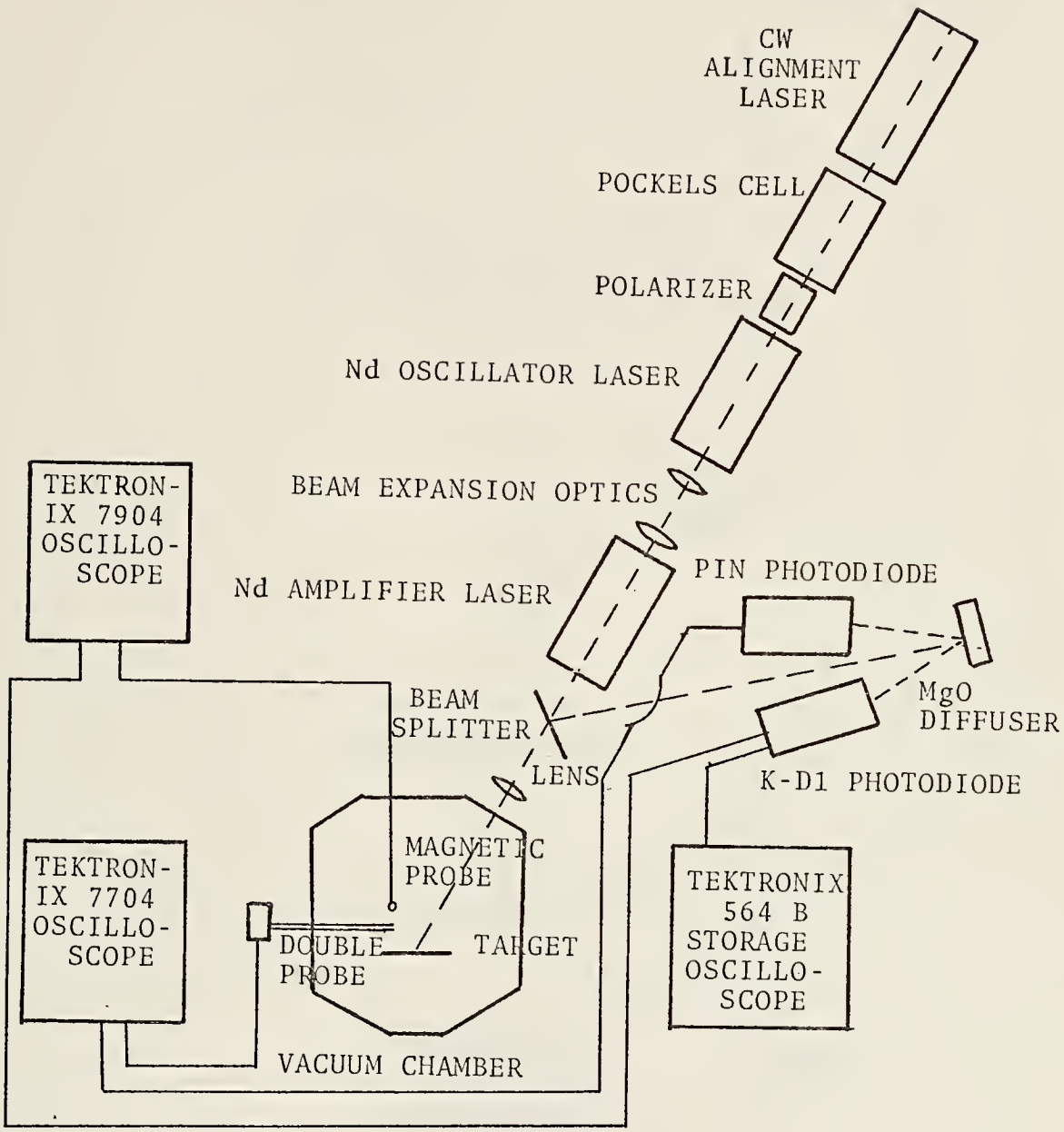

Figure 1. Experimental Arrangement.

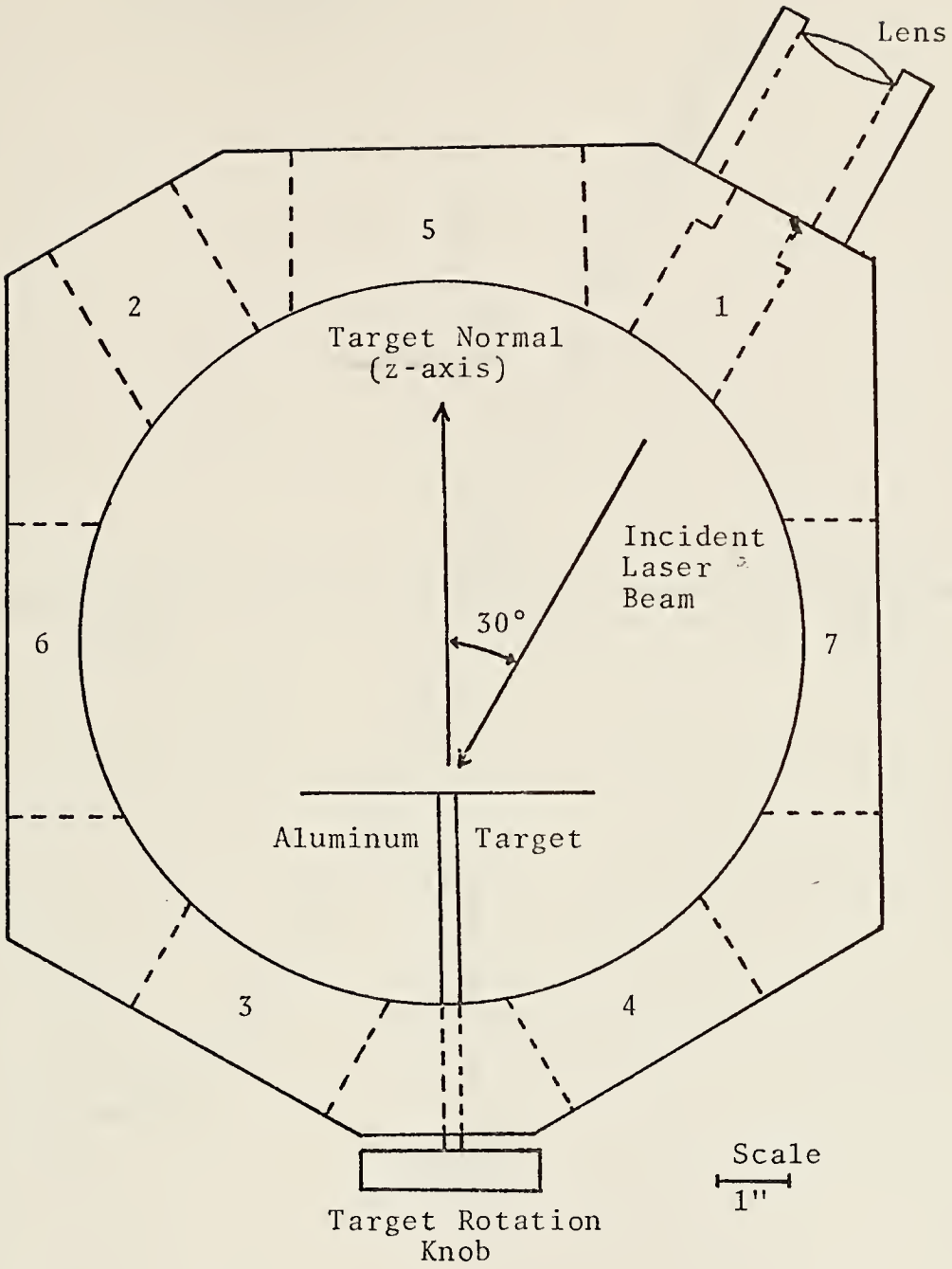

Figure 2. Top View of Vacuum Chamber. Port 1 is the Laser Beam Entry Port, Ports 2 to 7 are observation Ports.

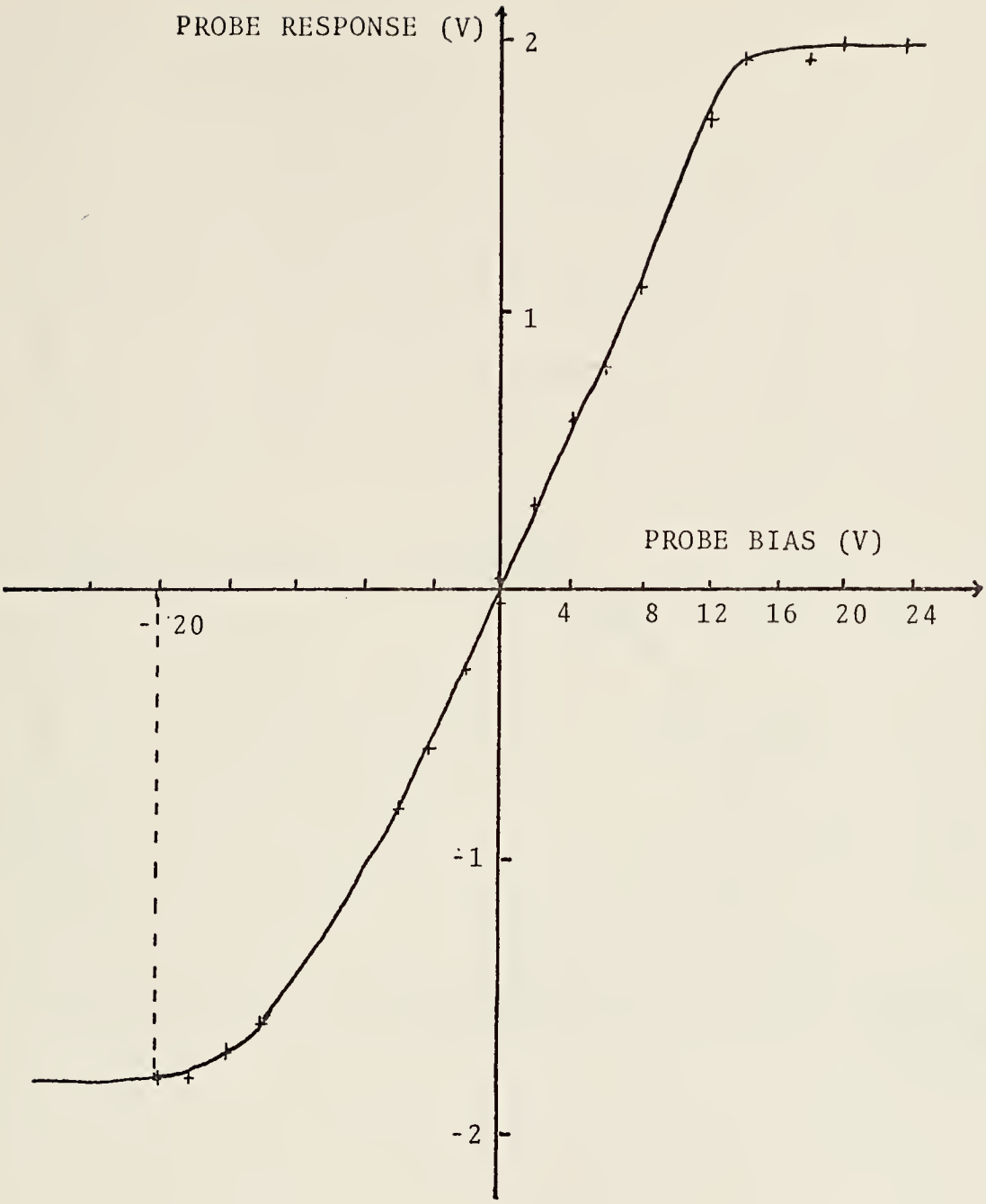

Figure 3. Electric Doubles Probe Characteristic at the Peak of the Early Time Signal.

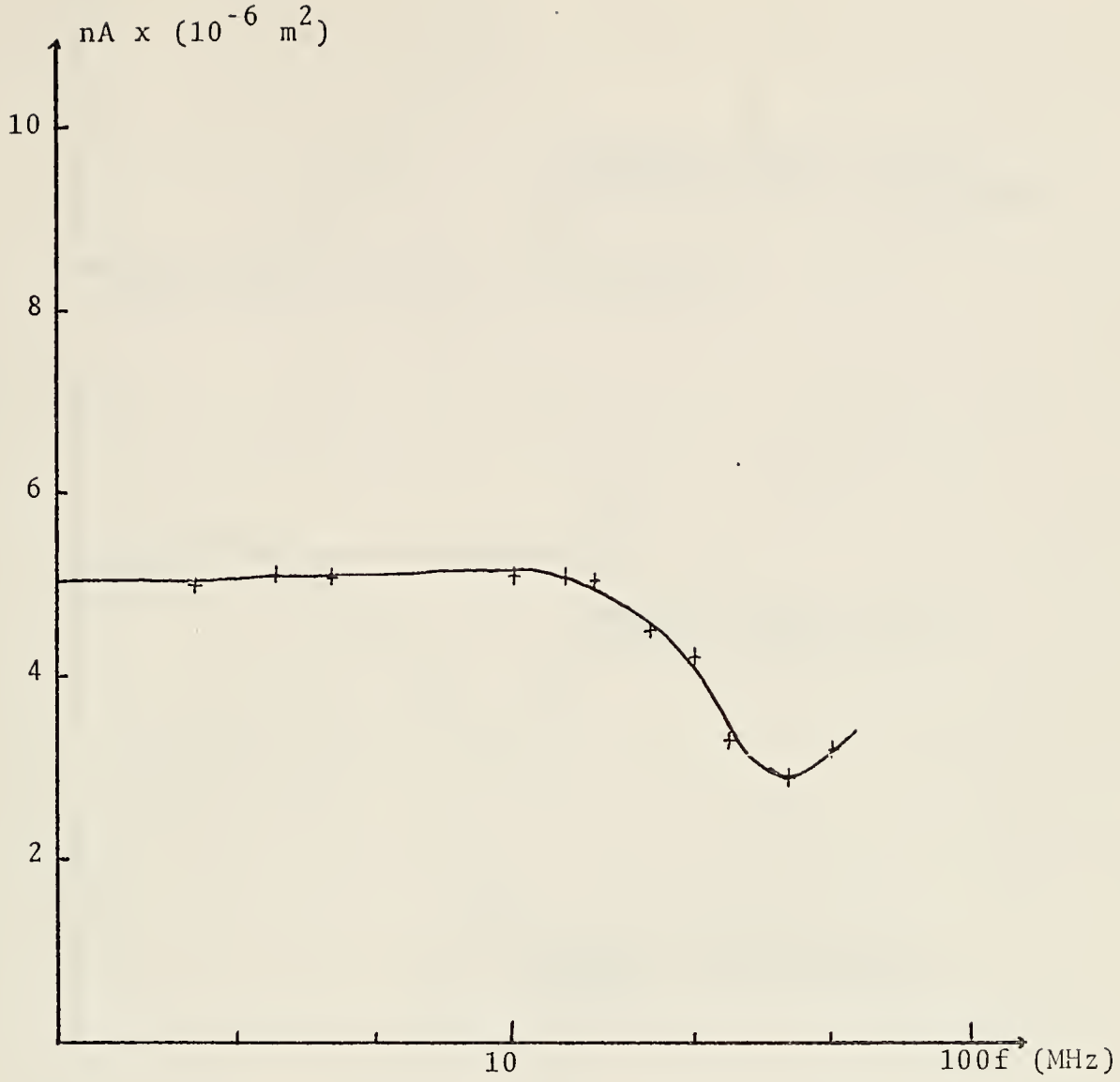

Figure 4. Calibration Curve for the Magnetic Probe.

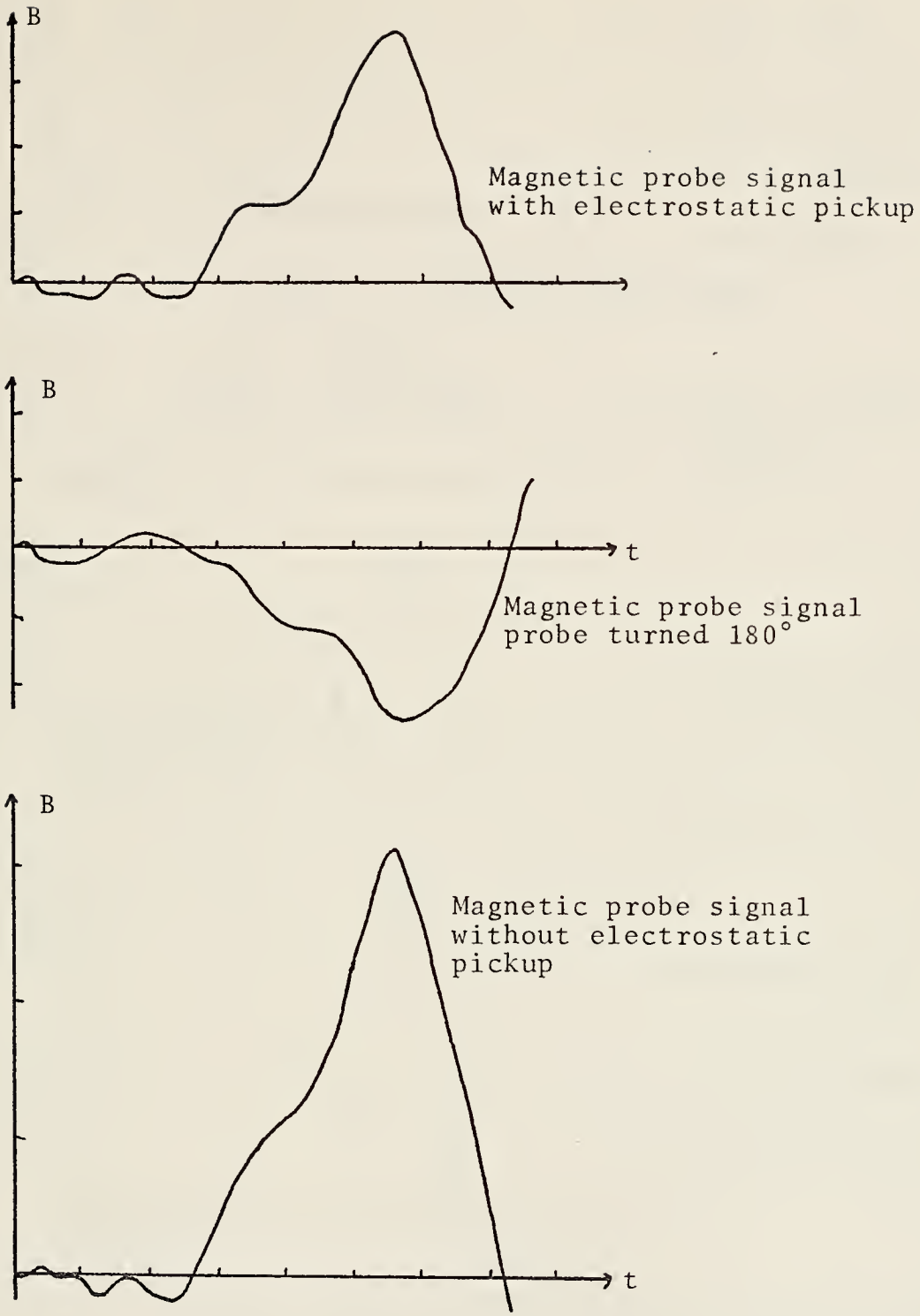

Figure 6. Removal of electrostatic Pickup from Magnetic Probe Signal. (4 Gauss/20 nsec per division)

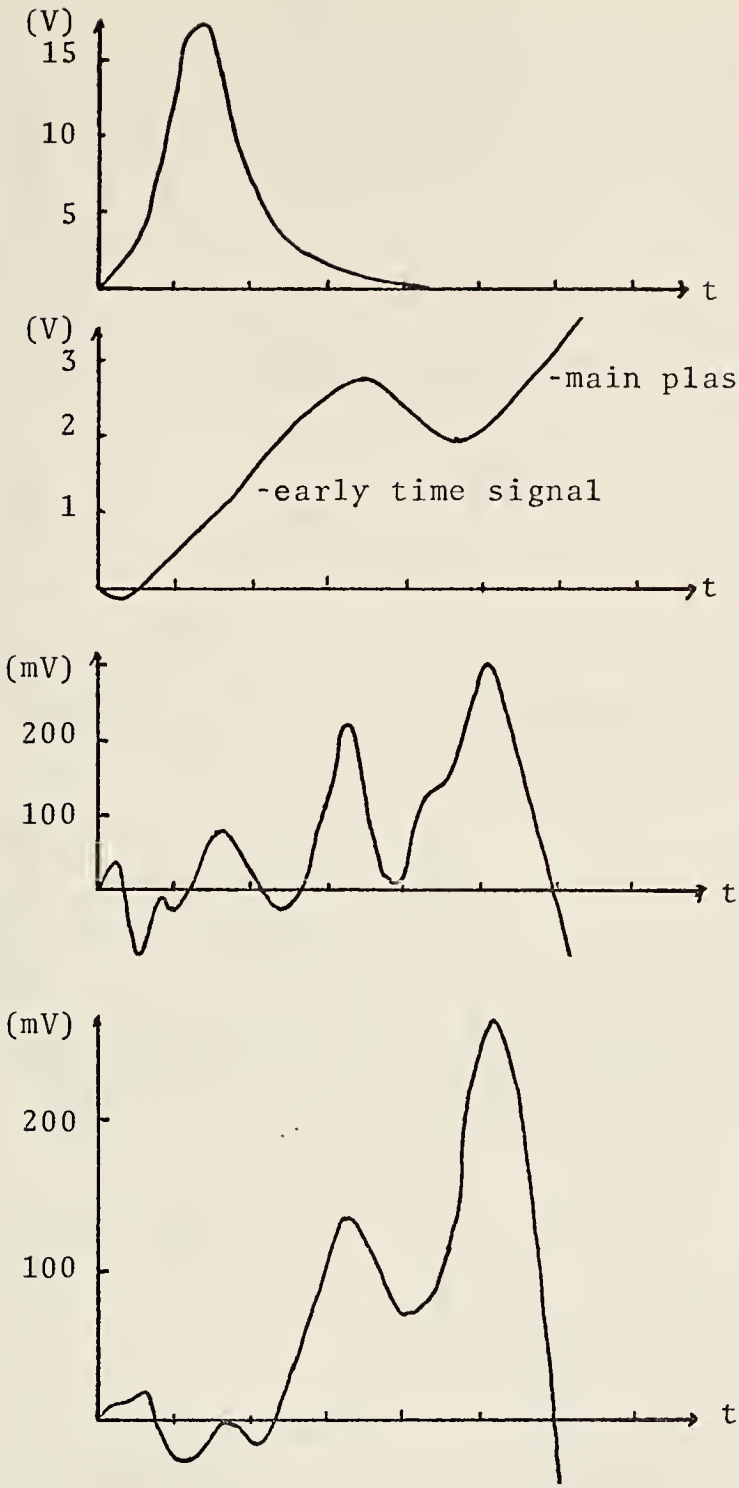

a) Laser pulse t=0, time the leading edge of laser pulse hits the target.

b) Double probe signal.

c) Magnetic probe signal $\partial B/\partial T$

d) Magnetic probe signal $\partial B/\partial T$ with electrostatic pickup removed

Figure 7. Temporal relationship between laser pulse, double probe signal and magnetic probe signal. Probe position (0.4,0,1.0). (Time scale 20 nsec per division)

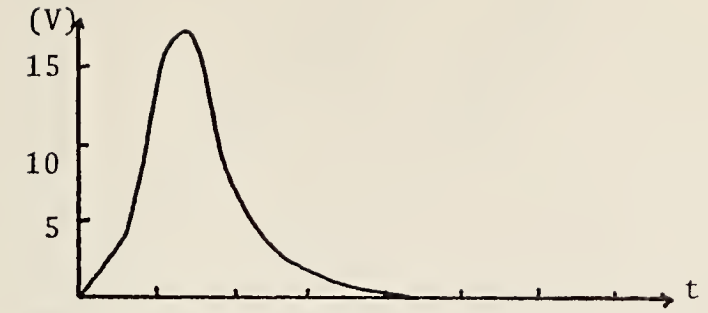

a) Laser pulse

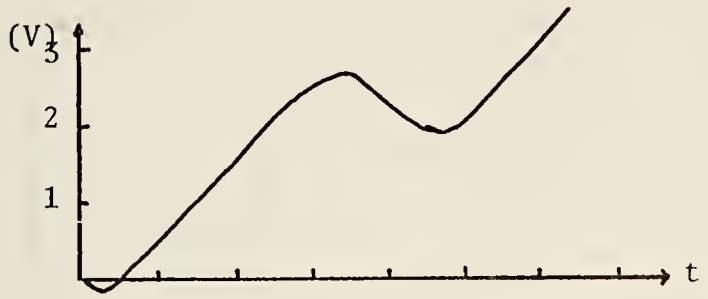

b) Double probe signal

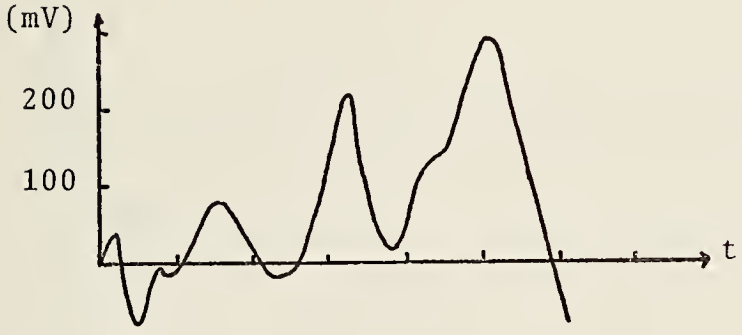

c) Magnetic probe signal $\partial B/\partial t$

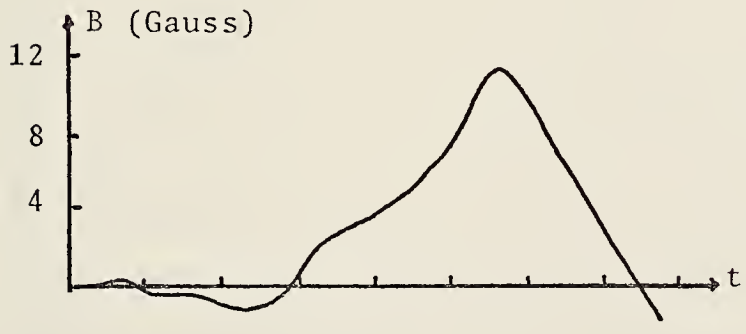

d) Magnetic probe signal (integrated)

Figure 8. Temporal relationship between laser pulse, double probe signal and integrated and non-integrated magnetic probe signal for probe position (0.4,0,1.0). (Time scale 20 nsec per division)

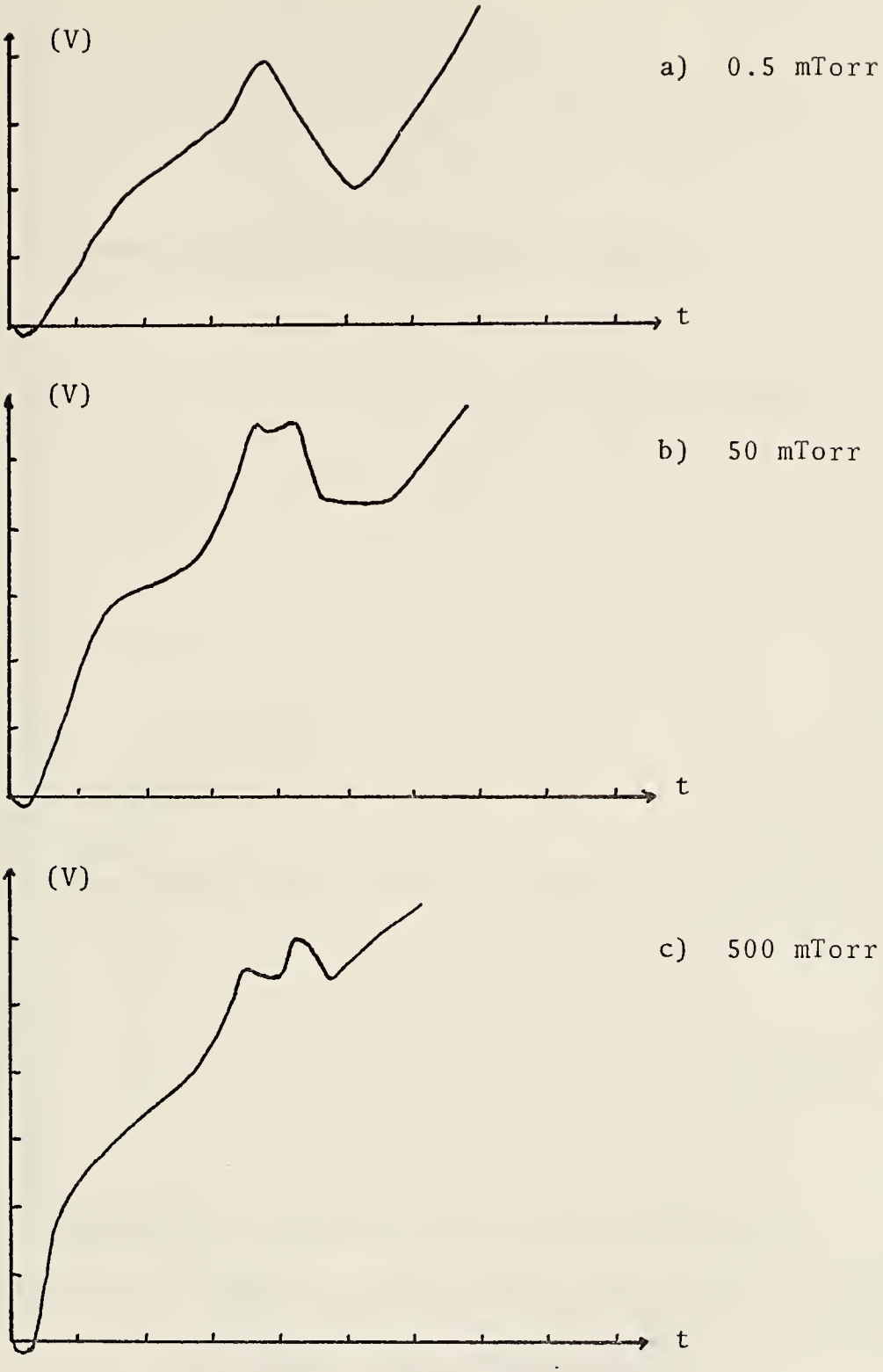

Figure 9. Early time signal from electric double probe in different nitrogen background pressures. Probe position (0.4,0,1.0). (1V/20 nsec per division).

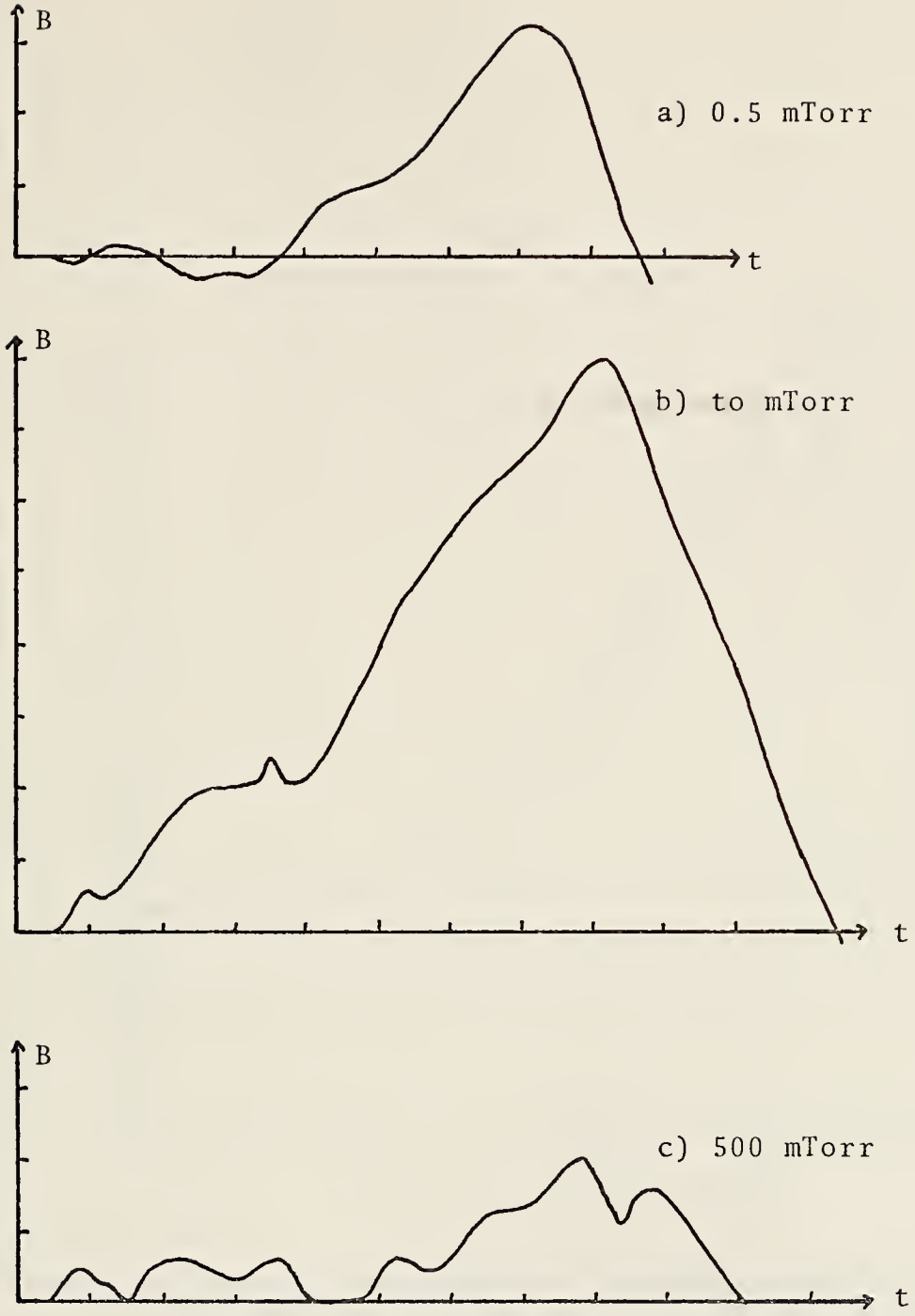

Figure 10. Magnetic probe signal in nitrogen background pressure of a) 0.5 mTorr, b) 50 mTorr and c) 500 mTorr for probe position (0.4,0,1.0). (2 Gauss/20 nsec per division).

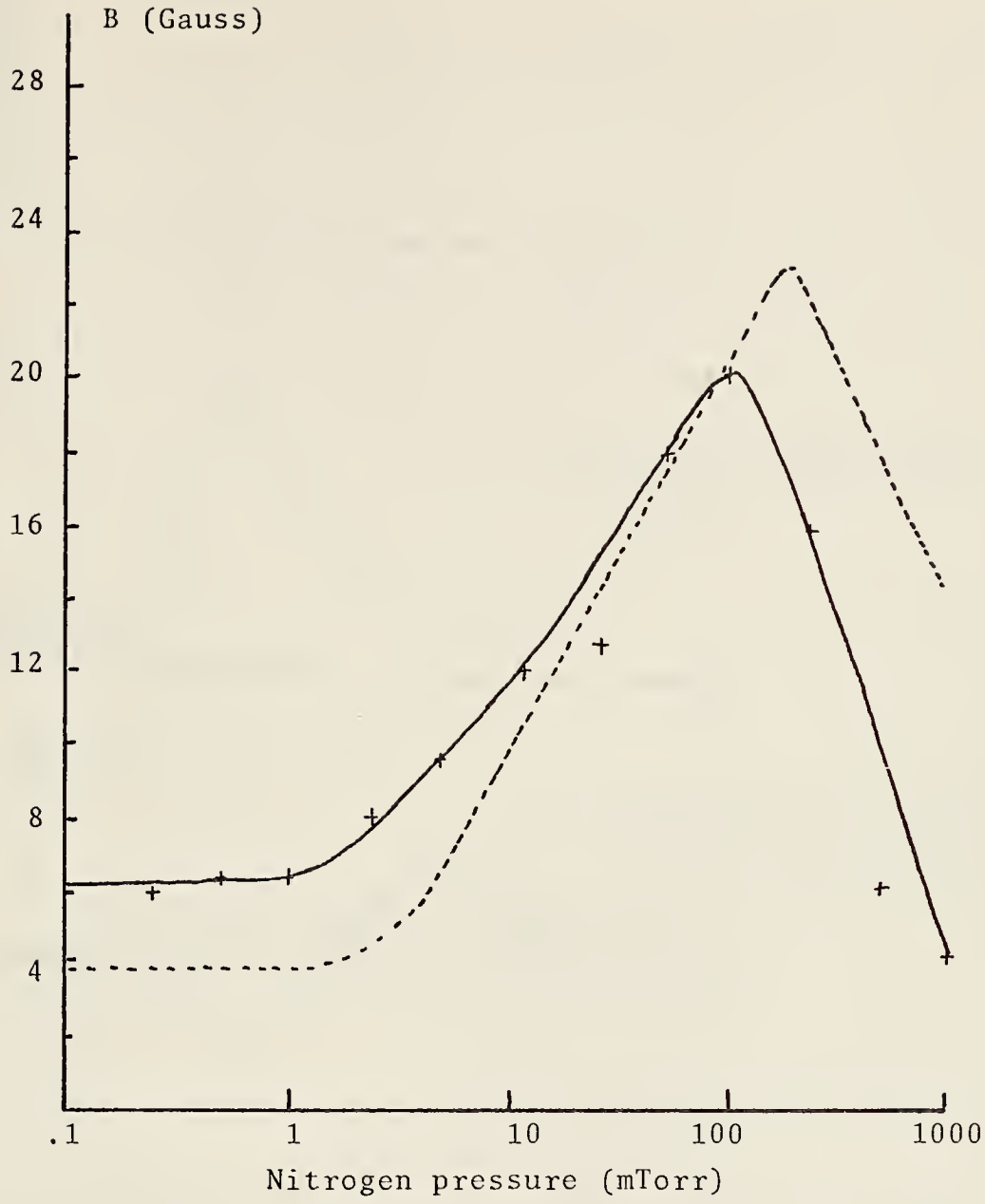

Figure 11. Pressure dependence of azimuthal magnetic field for position (0.4,0,1.0) (solid curve), and for position (0.3,0,0.4) (dashed curve). Dashed curve scaled down 1:10.

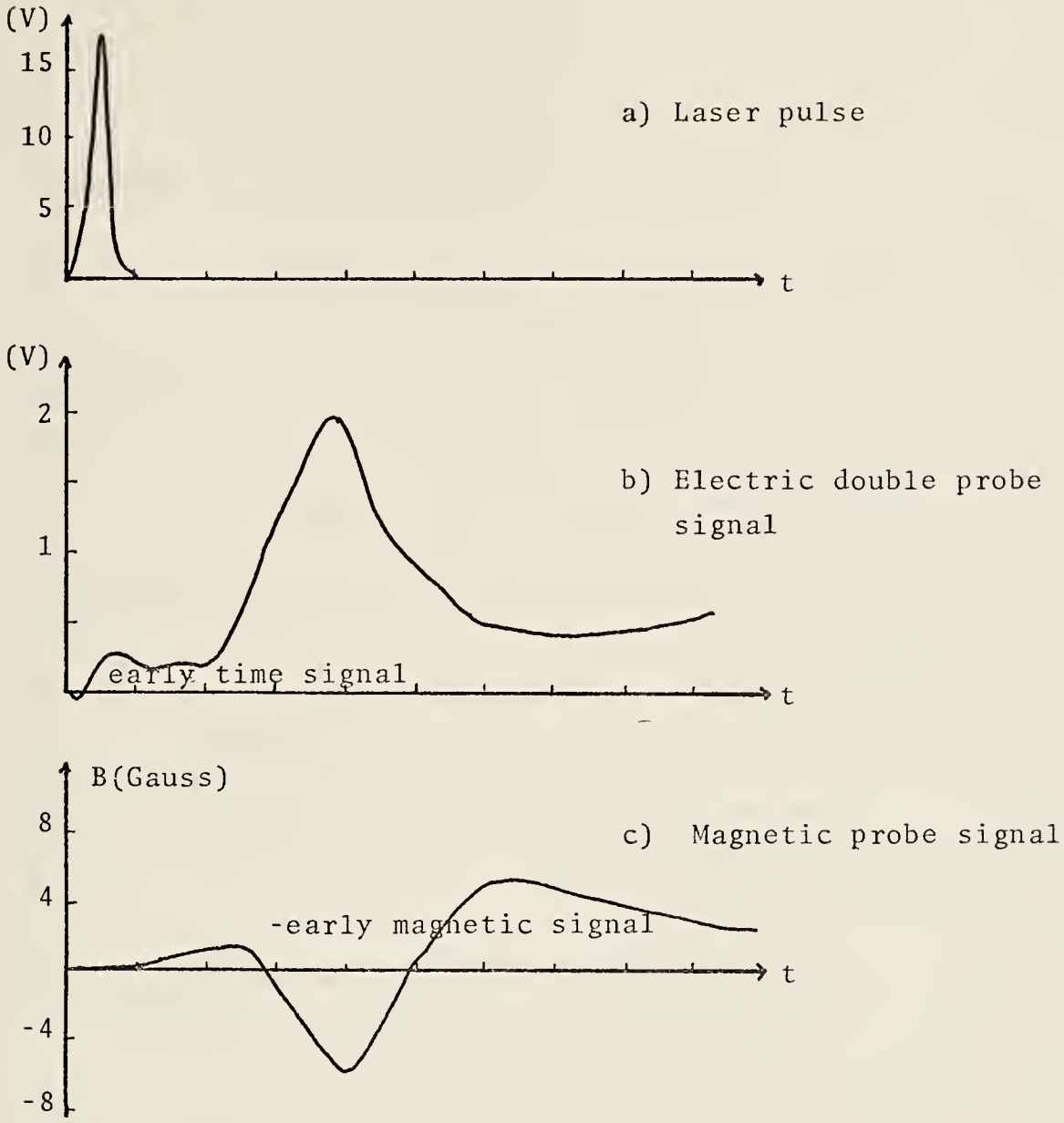

Figure 12. Temporal relationship between laser pulse electrice double probe signal and magnetic probe signal in vacuum for (0.6,0,2.5). (Time scale 100 nsec per division).

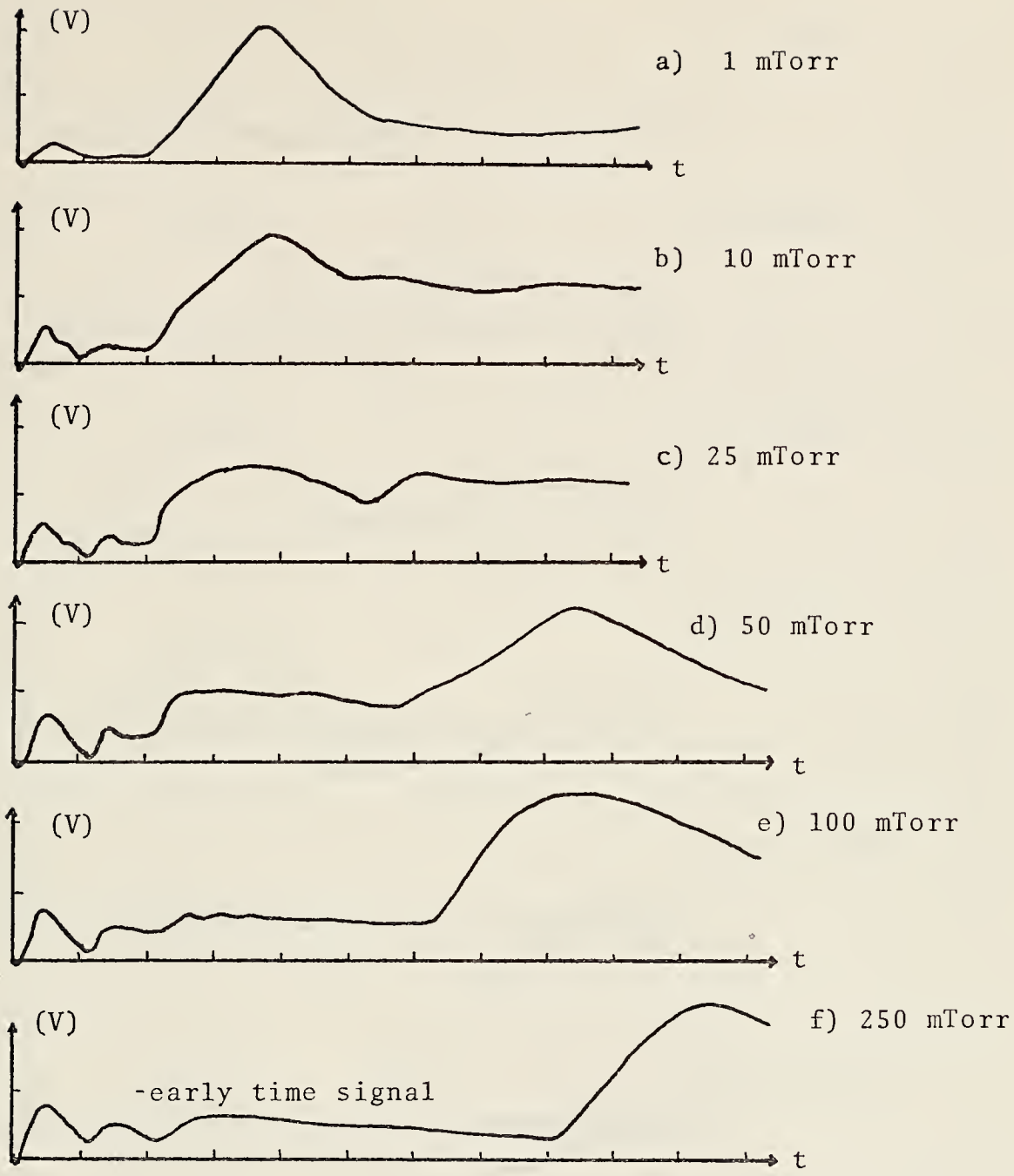

Figure 13. Electric double probe signal for different background pressure for (0.6,0,2.5). (1V/100 nsec per division.)

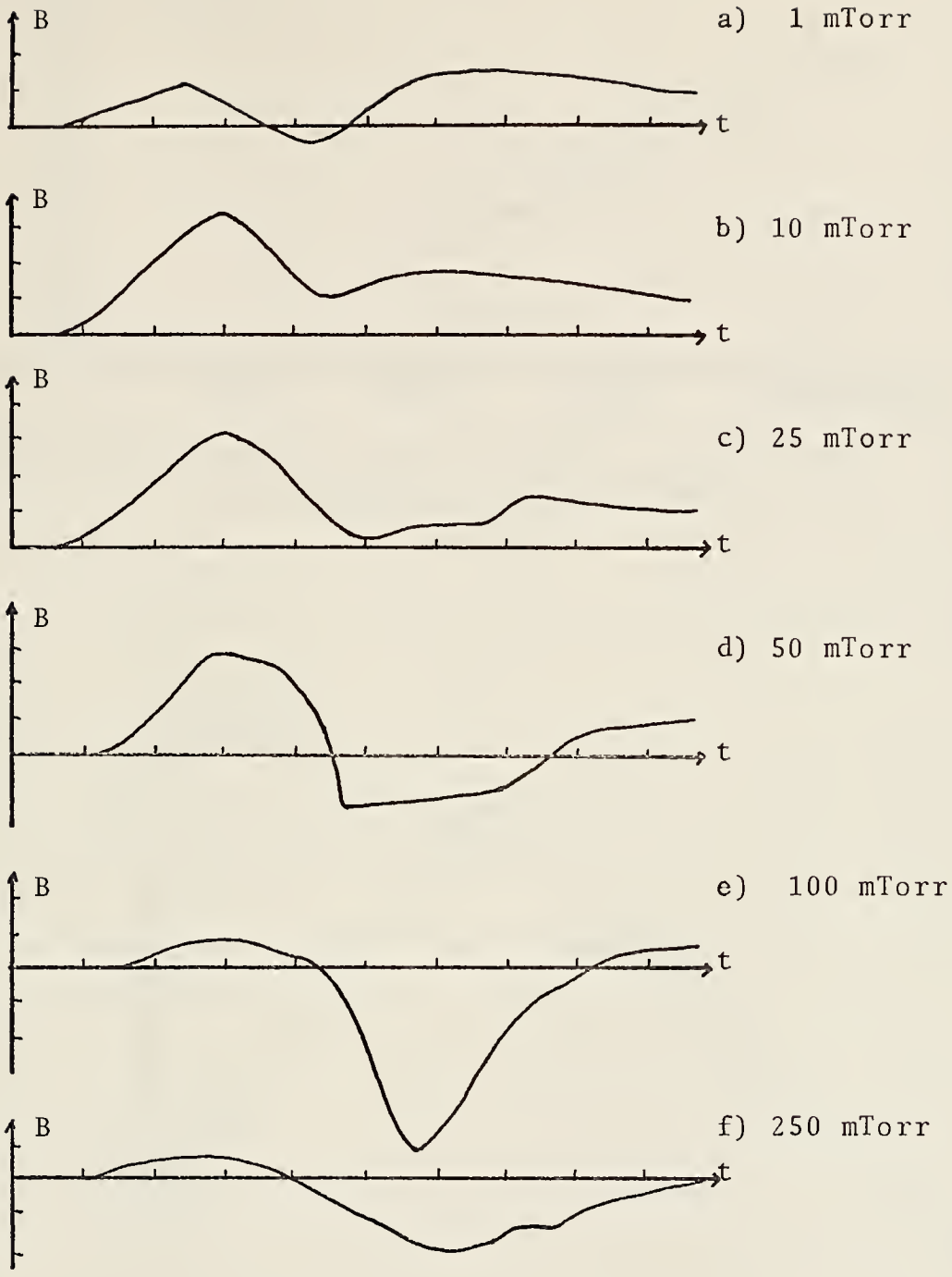

Figure 14. Magnetic probe signal for different background pressures of nitrogen. Probe position (0.6,0,2.5) (4 Gauss/100 nsec per division).

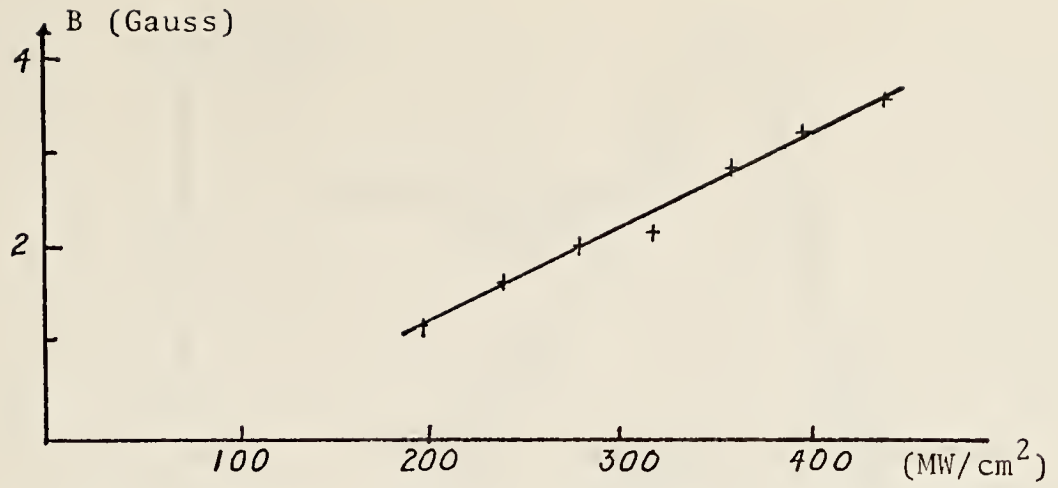

Figure 15. Magnetic field strength as function of irradiance for probe position (0.6,0,2.5).

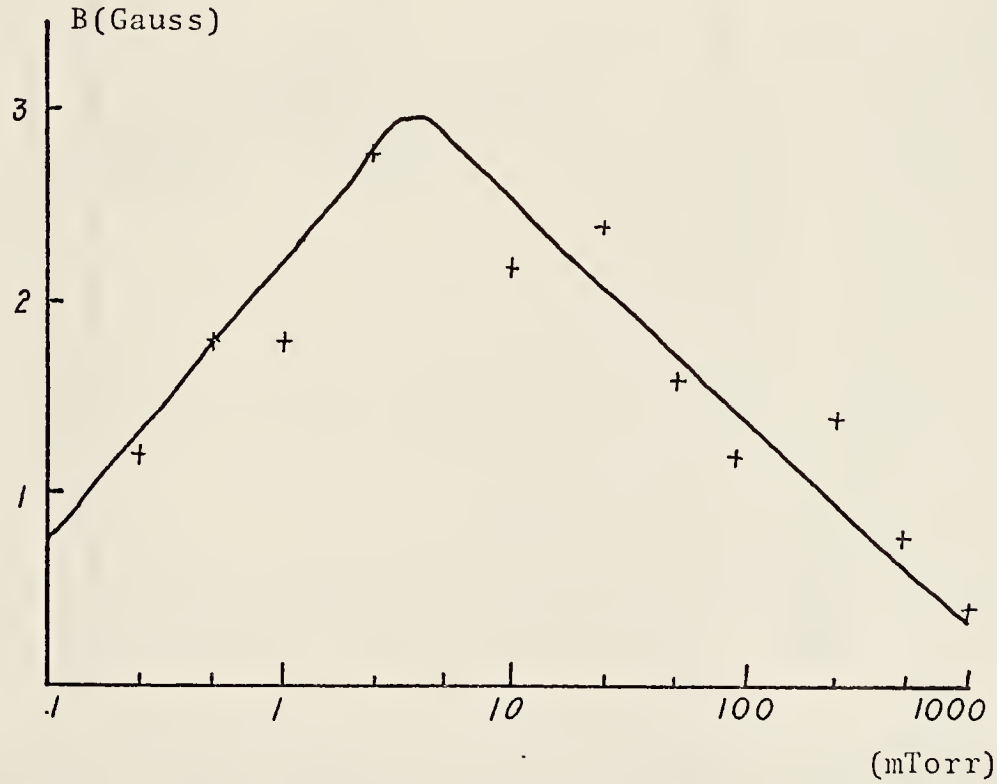

Figure 16. Maximum early magnetic signal as function of nitrogen background pressure for (0.6,0,2.5)

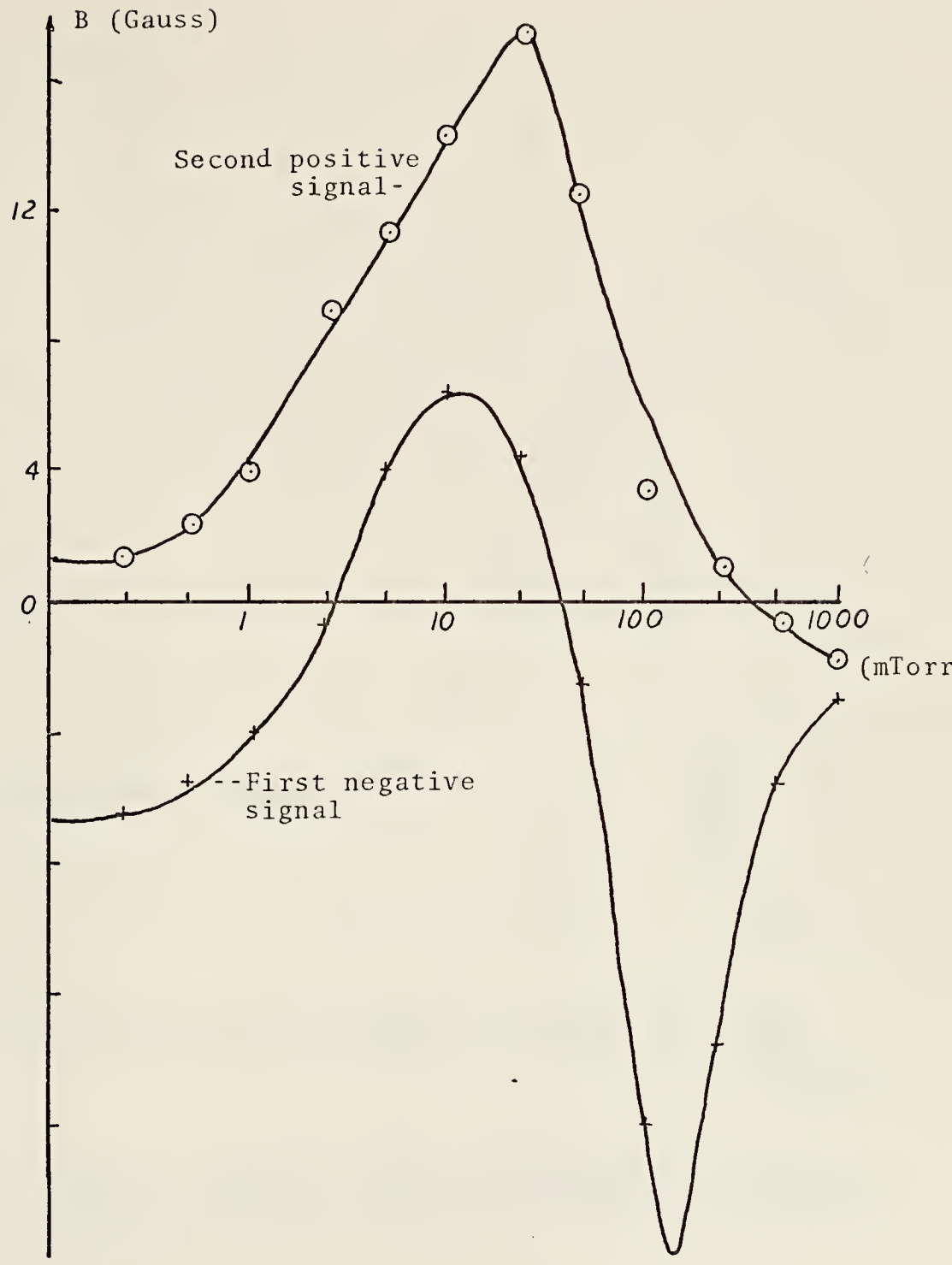

Figure 17. First negative magnetic signal and second positive magnetic signal as function of nitrogen background pressure for (0.6,0,2.5)

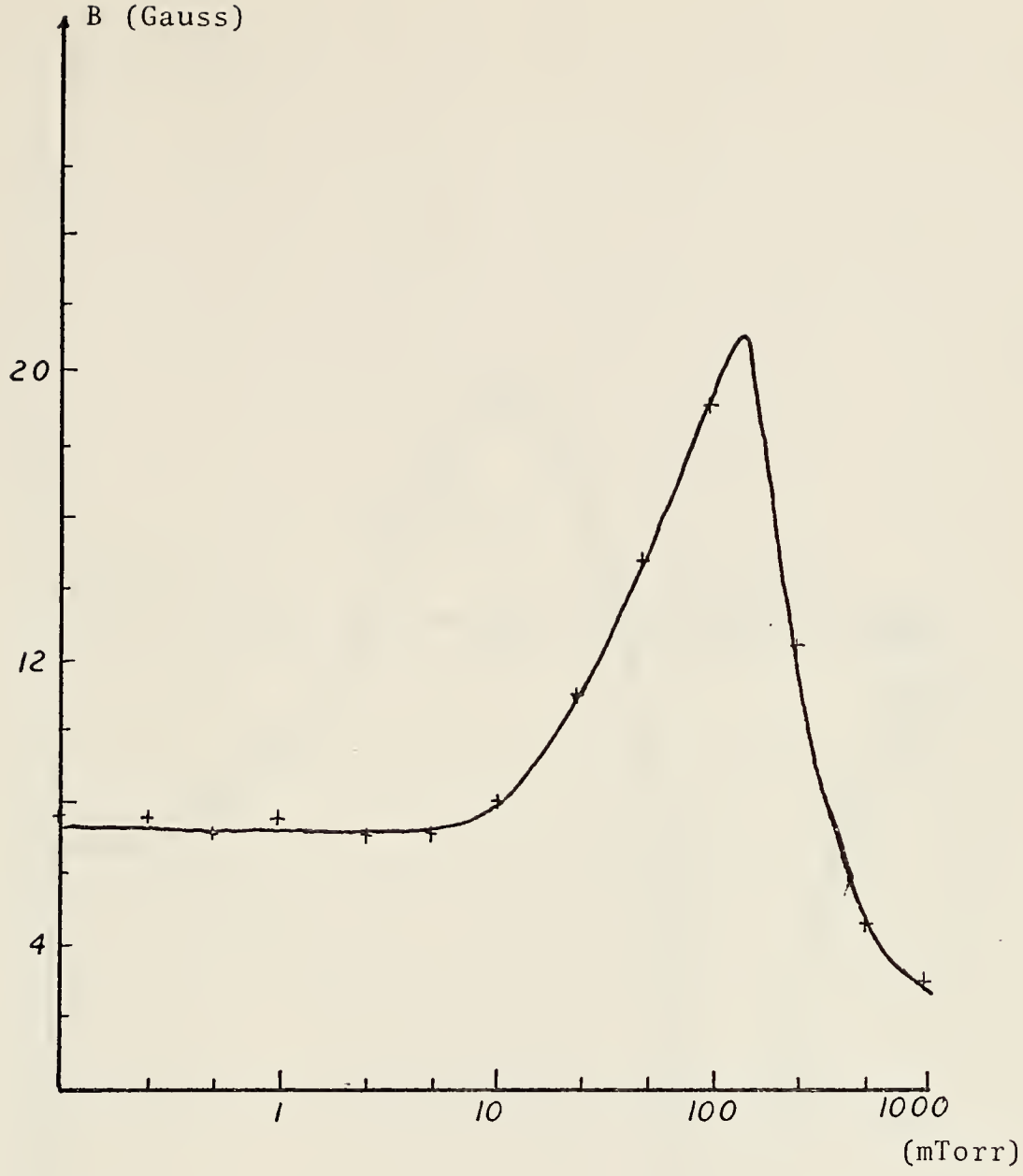

Figure 18. Negative magnetic signal subtracted from positive magnetic signal as function of nitrogen background pressure for (0.6,0,2.5).

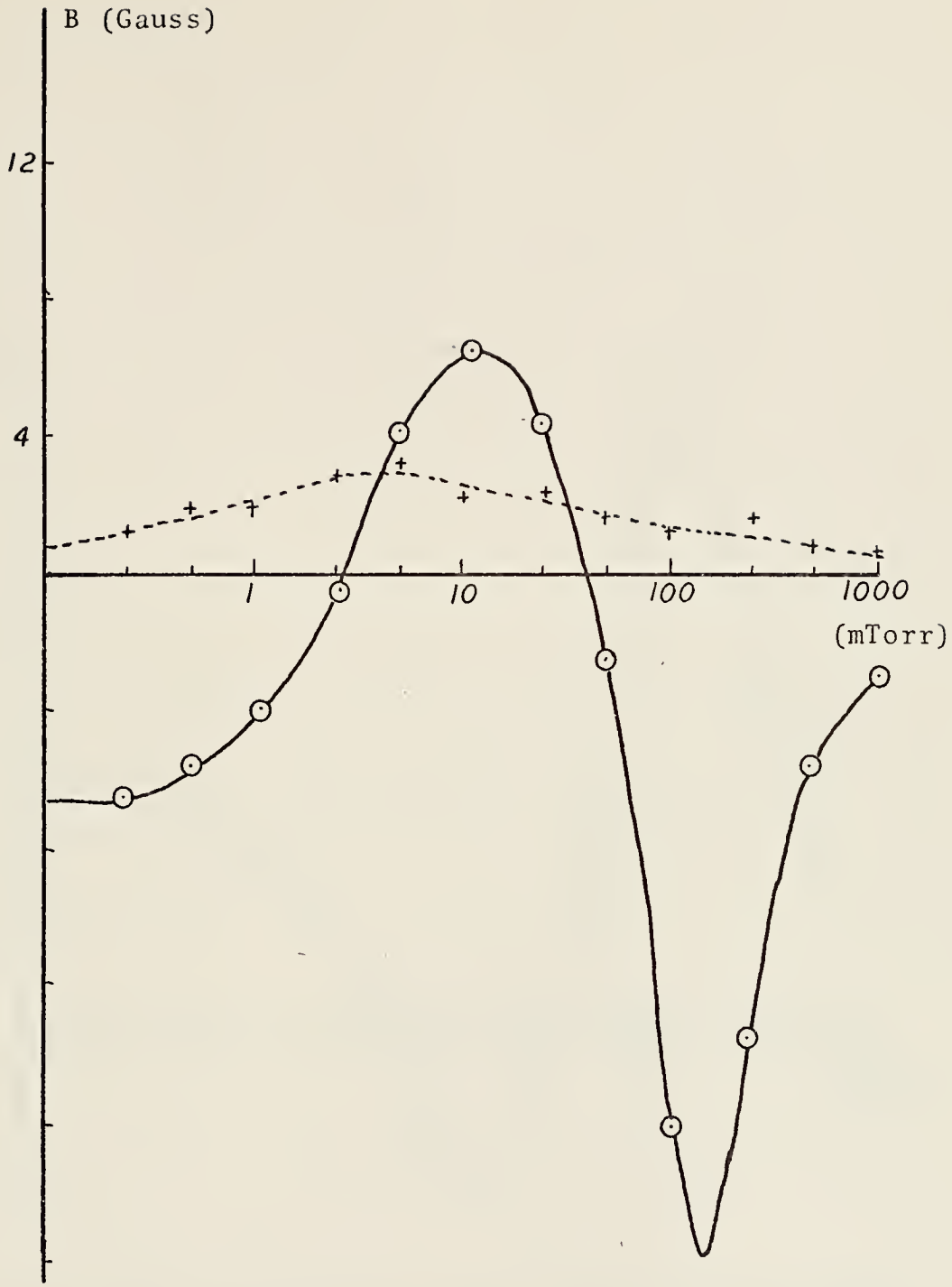

Figure 19. Early magnetic signal and negative magnetic signal as function of nitrogen background pressure for (0.6,0,2.5).

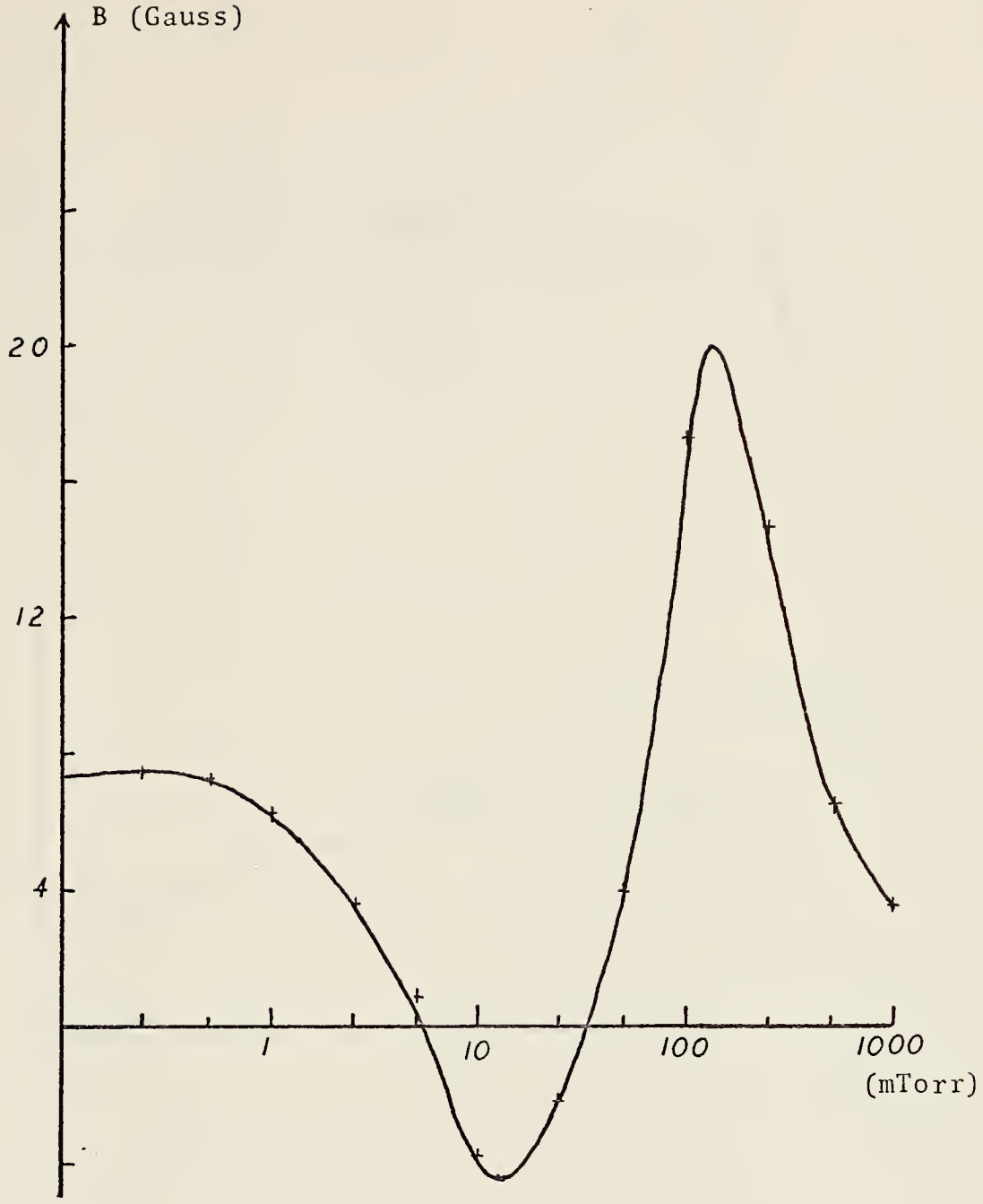

Figure 20. Negative magnetic signal subtracted from early magnetic signal as function of nitrogen background pressure for (0.6,0,2.5).

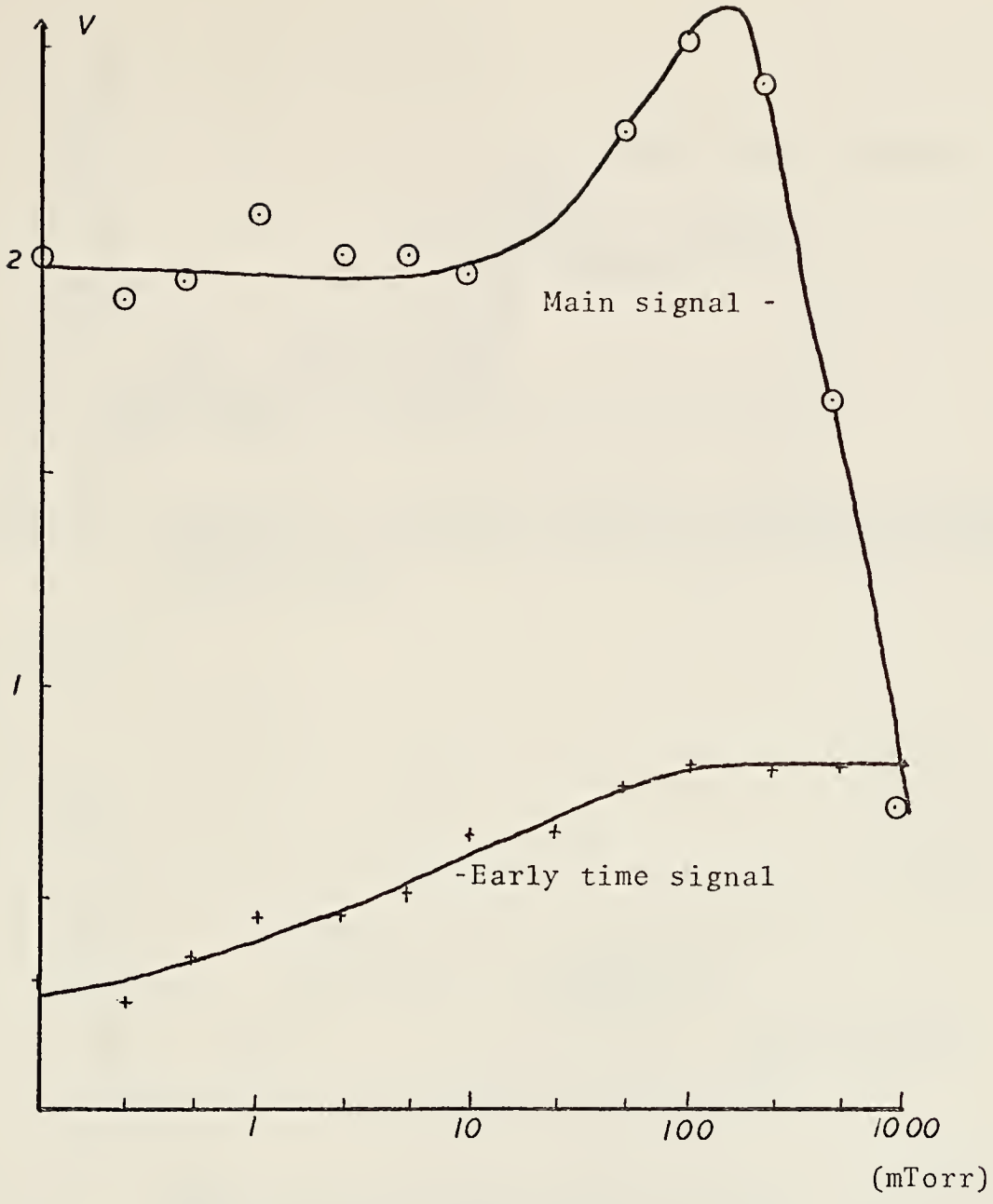

Figure 21. Early time signal and main signal of electric double probe as function of background pressure for (0.6,0,2.5)

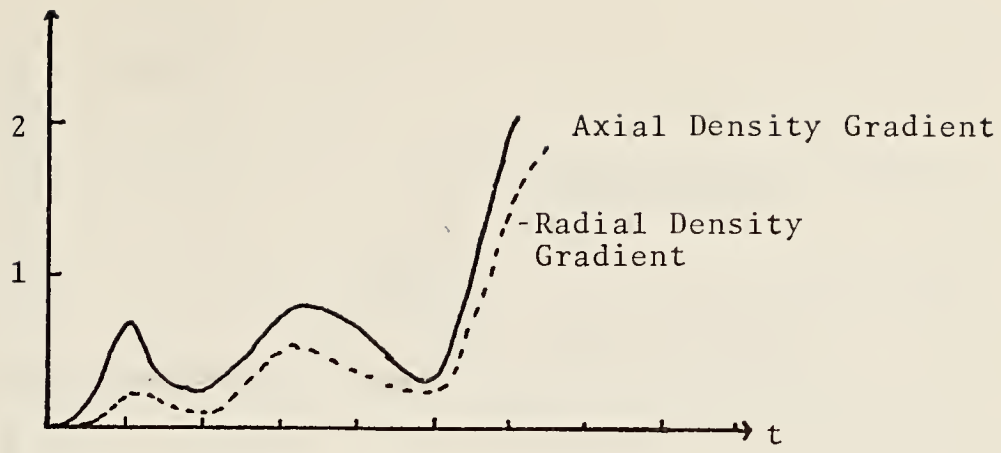

Figure 22. Magnitude of Density Gradient in Radial and Axial Direction for (0.4,0,1.0) (relative units/20 nsec per division)

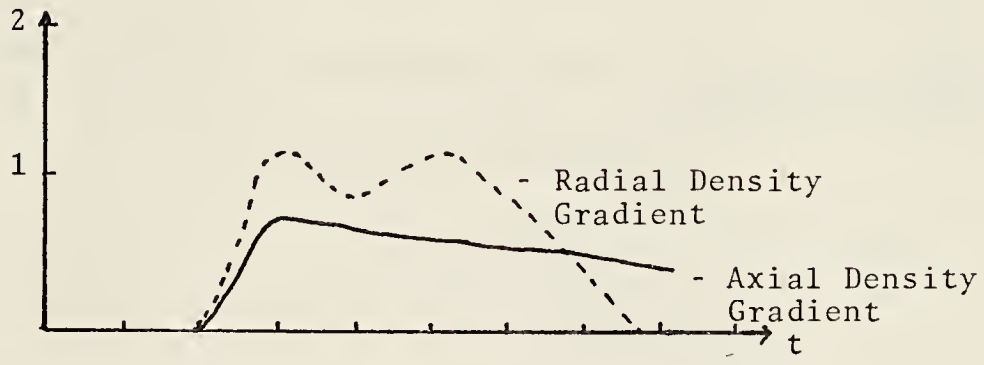

Figure 23. Magnitude of Density Gradient in Radial and Axial Direction for (0.6,0,2.5) in Vacuum. (Relative units/100 nsec per division)

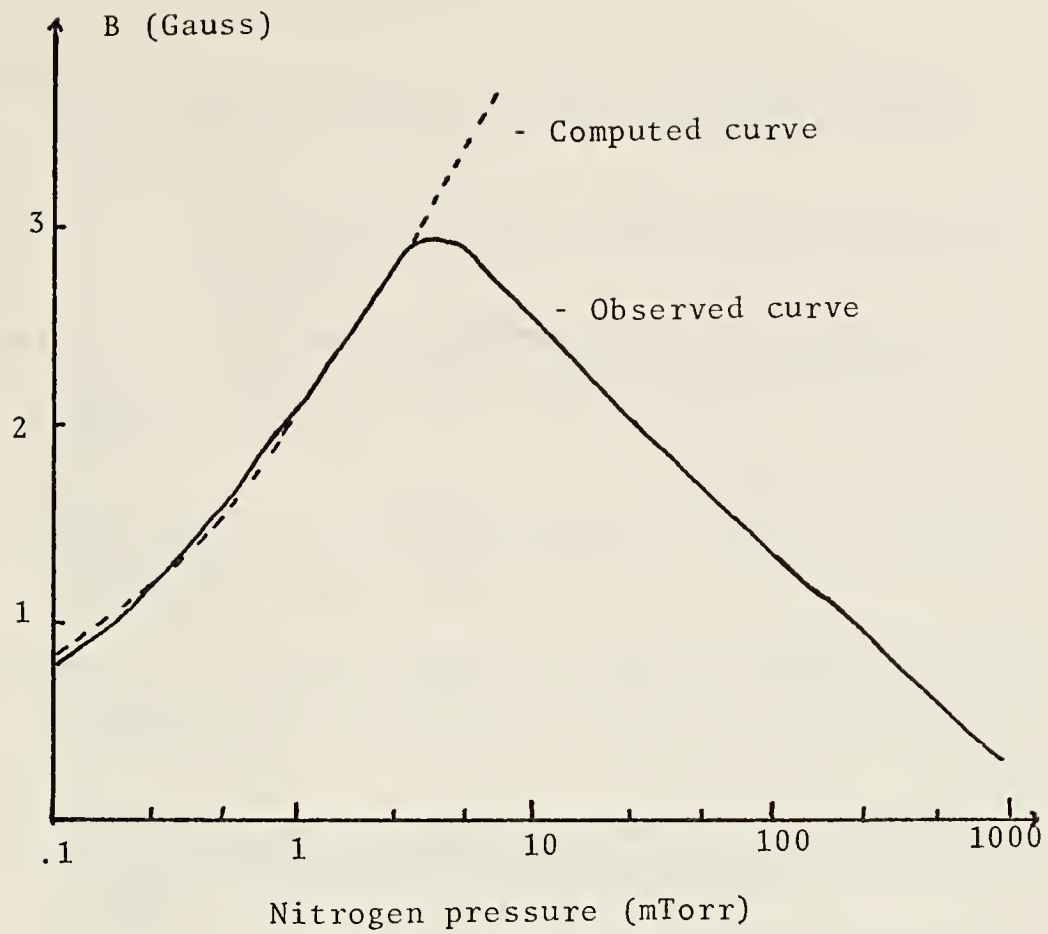

Figure 24. The maximum observed (solid line) and computed (dashed line) values for $B_{\theta MAX}$ for the early magnetic signal as a function of nitrogen background pressure for (0.6,0,2.5)

BIBLIOGRAPHY

1. DeMichelis, C., "Laser-Interaction with Solids--A Bibliographical Review," IEEE Journal of Quantum Electronics, v. 6, no. 10, p. 630-641, October 1970.

2. Ready, J. F., Effects of High-Power Laser Radiation, Academic Press, 1971.

3. Mulser, R., Sigel, R., Witkowski, S., "Plasma Production by Laser," Physics Reports (Section C of Physics Letters) 6, no. 3, p. 187-239, 14 June 1972.

4. Korobkin, V. V. and Serov, R. V., "Investigation of the Magnetic Field of a Spark Produced by Focusing Laser Radiation," JETP Letters, v. 4, no. 3, p. 102-106, 1 August 1966.

5. Stamper, J. A. and others, "Spontaneous Magnetic Fields in Laser-Produced Plasmas," Physical Review Letters, v. 26, no. 17, p. 1012-1015, 26 April 1971.

6. McKee, L. L., An Investigation of the Self-Generated Magnetic Fields Associated with a Laser Produced Plasma, Ph.D. Thesis, Naval Postgraduate School, 1972.

7. Bird, R. S., The Pressure Dependence of Spontaneous Magnetic Fields in Laser Produced Plasmas, Ph.D. Thesis, Naval Postgraduate School, 1973.

8. Honig, R. E. and Woolston, J. R., "Laser-Induced Emission of Electrons, Ions, and Neutral Atoms from Solid Surfaces," Applied Physics Letters, v. 2, no. 7, p. 138-139, 1 April 1963.

9. Honig, R. E., "Laser-Induced Emission of Electrons and Positive Ions from Metals and Semiconductors," Applied Physics Letters, v. 3, no. 1, 1 July 1963.

10. Brooks, K. R., An Investigation of Early Disturbances Found in Association with Laser-Produced Plasmas, MS Thesis, Naval Postgraduate School, 1973.

11. Chase, J. B., LeBlanc, J. M., and Wilson, J. R., "Role of Spontaneous Magnetic Fields in a Laser-Created Deuterium Plasma," The Physics of Fluids, v. 16, no. 7, p. 1142-1148, July 1973.

12. Koopman, D. W., "Precursor Ionization Fronts Ahead of Expanding Laser-Plasmas," Phys. Fluids, v. 15, no. 1, p. 56-62, January 1972.

13. Engelhardt, A. G., and others, "Linear and Nonlinear Behavior of Laser Produced Aluminum Plasmas," Phys. Fluids, v. 13, no. 1, p. 212-213, 1970.

14. Bykovskii, Y. A. and others, "Mass-Sprectrometer Investigation of Ions Formed by Interaction Between Laser Radiation and Matter," Soviet Physics - Technical Physics, v. 13, no. 7, p. 986-988, January 1968.

15. Bykovskii, Y. A. and others, "Energy Distribution of the Ions by a Large Laser Pulse on a Solid Target," Soviet Physics - Technical Physics, v. 14, no. 9, p. 1269-1271, March 1970.

16. Bykovskii, Y. A. and others, "Formation of the Energy Spectrum of the Ions of a Laser Plasma," JETP Letters, v. 15, no. 6, p. 217-220, 20 March 1972.

17. Paton, B. E., and Isenor, N. R., "Energies and Quantities in Laser-Produced Metal Plasmas," Canadian Journal of Physics, v. 46, no. 10, p. 1237-1239, 1968.

18. Demtroeder, W. and Jantz, W., "Investigation of Laser-Produced Plasmas from Metal Surfaces," Plasma Physics, v. 12, no. 9, p. 691-703, 1970.

19. Allen, F. J., "Method of Determining Ion Temperatures in Laser-Produced Plasmas," Journal of Applied Physics, v. 41, no. 7, p. 3048-3051, June 1970.

20. Haught, A. F. and Polk, D. H., "Formation and Heating of Laser Irradiated Solid Particle Plasmas," Phys. Fluids, v. 13, no. 11, p. 2825-2841, November 1970.

21. Irons, F. E., McWhirter, R. W. P., and Peacock, N. J., "The Ion Velocity Structure in a Laser Produced Plasma," Journal of Physics B, v. 5, no. 10, p. 1975-1987, October 1972.

22. Mulser, P., "Electrostatic Fields and Ion Separation in Expanding Laser Produced Plasmas," Plasma Physics, v. 13, no. 11, p. 1007-1012, 1971.

23. Allen, F. J., "Production of High-Energy Ions in Laser Produced Plasmas," Journal of Applied Physics, v. 43, no. 5, p. 2169-2175, May 1972.

24. Stumpfel, C. R., Robitaille, J. L., and Kunze, H. J., "Investigation of the Early Phases of Plasma Production by Laser Irradiation of Plane Solid Targets," Journal of Applied Physics, v. 43, no. 3, p. 902-907, March 1972.

25. Ehler, W. and Linlor, W. I., "Origin of Energetic Ions from Laser-Produced Plasmas," Journal of Applied Physics, v. 44, no. 9, p. 4229-4231, September 1973.

26. Davis, L. J., Self-Generated Magnetic Fields Produced by Laser Bombardment of a Solid Target, MS Thesis, Naval Postgraduate School, 1972.

27. McLaughlin, T. A., Inductive Magnetic Probe Diagnostics in a Plasma, MS Thesis, Naval Postgraduate School, 1970.

28. Basov, N. G. and others, "Heating and Decay of Plasma Produced by a Giant Laser Pulse Focused on a Solid Target," Soviet Physics JETP, v. 24, no. 4, p. 659-665, April 1967.

29. Naval Research Laboratory Report 7411, Laser-Induced Sources for Magnetic Fields, by J. A. Stamper, p. 1-10, 16 June 1972.

30. Schwirzke, F., Measurements of Spontaneous Magnetic Fields in Laser Produced Plasmas, paper presented at the Third Workshop on "Laser Interaction and Related plasma Phenomena," Rensselaer Polytechnic Institute, Troy, New York, August 13-17, 1973.

31. Stamper, J. A., "Magnetic Field Generation due to Radiation Pressure in a Laser-Produced Plasma," Phys. Fluids, v. 16, no. 11, p. 2024-2025, Nov. 1973.

32. Dean, S. O. and others, "Demonstration of Collisionless Interactions Between Interstreaming Ions in a Laser-Produced-Plasma Experiment," Physical Review Letters, v. 27, no. 8, p. 487-490, 23 August 1971.

33. Wright, T. P., "Comments on 'Demonstration of Collisionless Interactions Between Interstreaming Ions in a Laser-Produced-Plasma Experiment'," Physical Review Letters, v. 28, no. 5, p. 268-270, 31 January 1972.

34. Koopman, D. W., "Momemtum Transfer Interaction of a Laser Produced Plasma with a Low-Pressure Background," Phys. Fluids, v. 15, no. 11, p. 1959-1969, November 1972.

INITIAL DISTRIBUTION LIST

		No. Copies
1.	Defense Documentation Center Cameron Station Alexandria, Virginia 22314	2
2.	Library, Code 0212 Naval Postgraduate School Monterey, California 93940	2
3.	Professor A. W. Cooper, Code 61 Cr Department of Physics Naval Postgraduate School Monterey, California 93940	2
4.	Professor F. Schwirzke c/0 Dr. S. Witkowski Max-Planck-Institut für Plasmaphysik 8046 Garching bei München West-Germany	1
5.	Marineamt -A1 294 Wilhelmshaven Federal Republic of Germany	1
6.	Dokumentations Zentrale der Bundeswehr (See) 53 Bonn Friedrich Ebert Allee 34 Federal Republic of Germany	1
7.	Lieutenant Commander B. Wegener, FGN c/o Günter Wegener 4458 Neuenhaus Freih.v.Stein Str. 10a West-Germany	1

21 JUN75 22140

153803

Thesis
W334 Wegener
c.1 Measurements of early magnetic fields in laser produced plasmas.

21 JUN75 22140

r

153803

Thesis
W334 Wegener
c.1 Measurements of early magnetic fields in laser produced plasmas.

thesW334
Measurements of early magnetic fields in
3 2768 001 95157 7
DUDLEY KNOX LIBRARY